NASA TECHNICAL MEMORANDUM

NASA TM X-64741

SCINTILLATOR HANDBOOK WITH EMPHASIS ON CESIUM IODIDE

By John L. Tidd, Joseph R. Dabbs, and Norman Levine
Program Development and HEAO Project Office

April 13, 1973

NASA

George C. Marshall Space Flight Center
Marshall Space Flight Center, Alabama

MSFC - Form 3190 (Rev June 1971)

TECHNICAL REPORT STANDARD TITLE PAGE

1. REPORT NO.	2. GOVERNMENT ACCESSION NO.	3. RECIPIENT'S CATALOG NO.
NASA TM X-64741		

4. TITLE AND SUBTITLE	5. REPORT DATE
Scintillator Handbook with Emphasis on Cesium Iodide	April 13, 1973
	6. PERFORMING ORGANIZATION CODE
7. AUTHOR(S)	8. PERFORMING ORGANIZATION REPORT #
John L. Tidd, Joseph R. Dabbs, and Norman Levine	
9. PERFORMING ORGANIZATION NAME AND ADDRESS	10. WORK UNIT NO.
George C. Marshall Space Flight Center Marshall Space Flight Center, Alabama 35812	11. CONTRACT OR GRANT NO.
	13. TYPE OF REPORT & PERIOD COVERED
12. SPONSORING AGENCY NAME AND ADDRESS	Technical Memorandum
National Aeronautics and Space Administration Washington, D. C. 20546	14. SPONSORING AGENCY CODE

15. SUPPLEMENTARY NOTES

Prepared by Program Development and HEAO Project Office

16. ABSTRACT

The objective of this report is to provide a background of reasonable depth and reference material on scintillators in general. Particular attention is paid to the cesium iodide scintillators as used in the High Energy Astronomy Observatory (HEAO) experiments. It is intended especially for use by persons such as laboratory test personnel who need to obtain a working knowledge of these materials and their characteristics in a short time.

EDITOR'S NOTE

Use of trade names or names of manufacturers in this report does not constitute an official endorsement of such products or manufacturers, either expressed or implied, by the National Aeronautics and Space Administration or any other agency of the United States Government.

17. KEY WORDS		18. DISTRIBUTION STATEMENT
Cesium iodide	Scintillation phosphors	Unclassified - unlimited
Scintillator	Phoswich materials	
Scintillation materials		Norman Levine
Scintillation detectors		
High energy particles		
Radiation detectors		

19. SECURITY CLASSIF. (of this report)	20. SECURITY CLASSIF. (of this page)	21. NO. OF PAGES	22. PRICE
Unclassified	Unclassified	91	NTIS

For sale by National Technical Information Service, Springfield, Virginia 22151

ACKNOWLEDGMENT

Appreciation is extended to the following organizations, which furnished portions of the data contained herein: The Harshaw Chemical Company, a Division of Kewanee Oil Company, Solon, Ohio; the University of California at San Diego (HEAO AGR-4 Experiment Group); NASA-Goddard Space Flight Center (HEAO ACR-6 Experiment Group), and the Materials Division of the Astronautics Laboratory, Marshall Space Flight Center.

TABLE OF CONTENTS

TABLE OF CONTENTS (Concluded)

LIST OF ILLUSTRATIONS

LIST OF ILLUSTRATIONS (Concluded)

LIST OF TABLES

TECHNICAL MEMORANDUM X-64741

SCINTILLATOR HANDBOOK WITH EMPHASIS ON CESIUM IODIDE

INTRODUCTION

A wide variety of methods exist which are useful for detecting and measuring cosmic radiation. Each method has unique advantages and disadvantages, and no one method is universally suitable for all applications. In general, more than one technique is applied and by correlating information, better accuracy and resolution of energy measurements are obtained.

Typical techniques useful for space application are listed as follows. This report is limited to the consideration of one subcategory, the inorganic scintillators.

1. Scintillation Detectors — Applicable for X Rays, Gamma Rays, and Charged Particles

    a. Inorganic Crystals.

    b. Plastic Materials.

    c. Liquids.

2. Cerenkov Detectors — Useful for Charged Particles Only

    a. Solids, i.e., Plastic, Glass, etc.

    b. Liquids.

    c. Gases.

3. Semiconductors — Useful for Ionizing Radiation

4. Ionizing Counters (Gas) — Useful for Ionizing Radiation

    a. Ion Chambers.

b. Proportional Counters.

c. Geiger-Mueller Counters.

d. Spark Chambers.

BASIC OPERATIONAL CHARACTERISTICS

To understand how well a scintillator performs its task of detecting radiation, it is necessary to consider the phases of the detection process. Figure 1 is a pictorial history of what happens when radiation impinges upon the crystal, and light of some wave number ν is radiated.

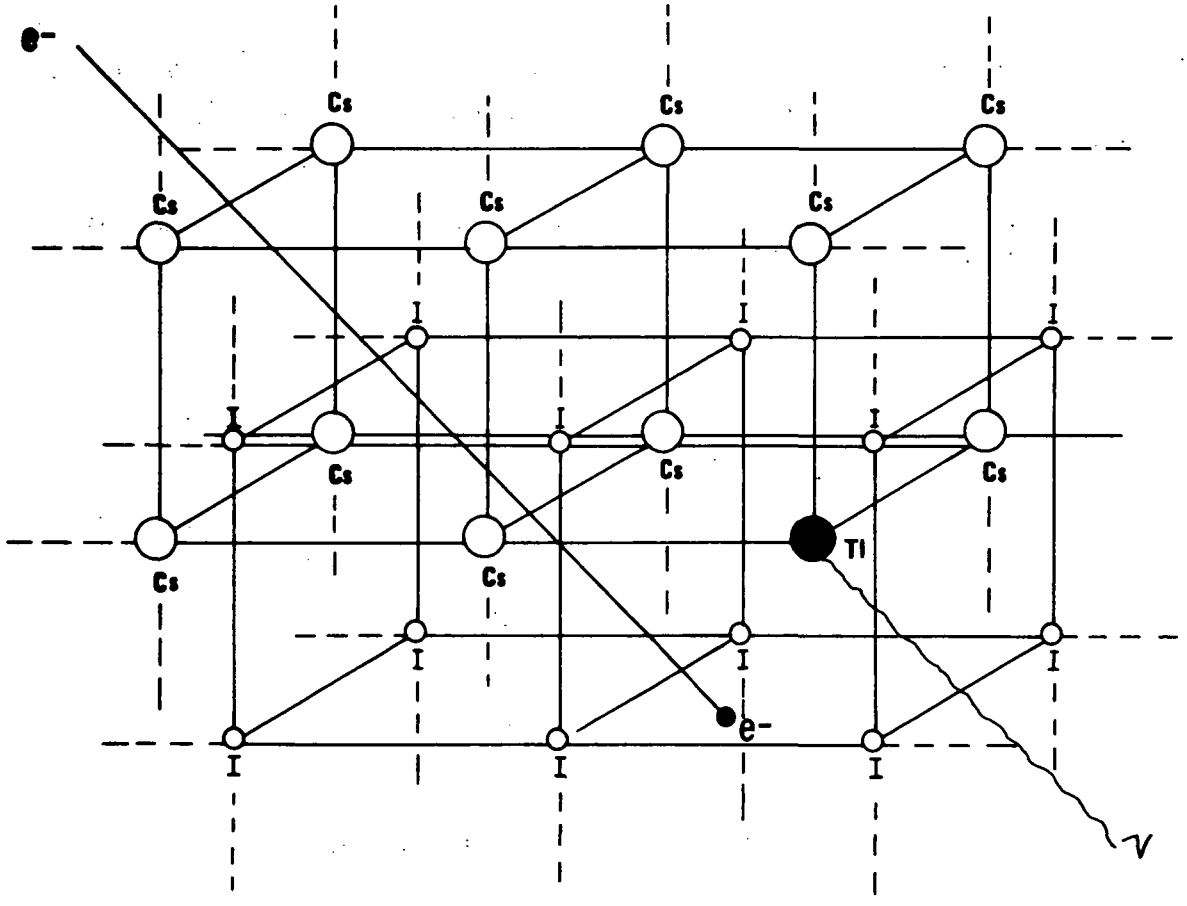

Figure 1. Crystal structure and scintillation mechanism of cesium iodide.

The charged particle moves through the crystal lattice and by coulomb interaction forces causes electrons in the valance band of the crystal to absorb energy. When these valance electrons return to their original state from the conduction band, energy is released by a number of mechanisms. Of common importance to these decay schemes is the existence of impurity levels in the lattice. To provide such deliberate crystal lattice imperfections is the purpose of the trace elements present as activation or "doping." The incident radiation, whether corpuscular (charged particle) or electromagnetic, must be made to lose some of its energy to the detector.

The absorption of charged particle (corpuscular) radiation differs fundamentally from that of electromagnetic radiation such as X rays and gamma rays as follows:

1. Charged particles dissipate their energy continuously in a sequence of many ionization and excitation events. The path of the particle in the scintillator is essentially straight, and the particle penetrates to a certain distance called the "range."

2. Electromagnetic radiation in the form of a well-collimated beam of X rays and/or gamma rays incident on a scintillator suffers a truly exponential attenuation:

a. Those collimated gamma rays which penetrate the scintillator have had no interaction.

b. Those which undergo single interactions are eliminated from the beam and deposit their energy as charged particles in the scintillator. The most important of the interactions which can occur are:

(1) The photoelectric effect.

(2) The Compton effect.

(3) Pair production.

The linear attenuation coefficient, μ, for the exponential absorption of electromagnetic radiation is made up additively of the linear coefficients corresponding to each of the three types of interactions and may be defined as

$$\mu_{\text{Total}} = \mu_{\text{Photoelectric}} + \mu_{\text{Compton}} + \mu_{\text{Pair Production}}$$

The mass attenuation coefficient is given by μ/ρ, where ρ is the density of the absorber. The dependence of μ_T on the incident energy E and the atomic number Z of the absorber is best expressed as follows:

$E < 0.5$ MeV	$0.5 \leq E \leq 5$ MeV	$E \geq 5$ MeV
Photoelectric effect dominant	Compton dominating	Pair production
$\mu_T \propto \rho Z^5$	$\mu_T \propto \rho Z$	$\mu_T \propto \rho Z^2$

Of course, the limits on E are general and will vary from scintillator to scintillator. For very high-energy gamma rays, the linear or total mass attenuation coefficient varies as Z^2 of the absorber since pair production is the dominant mode of energy dissipation.

When the scintillator is a mixture or compound of different elements whose mass attentuation coefficents are μ_1/ρ_1 , μ_2/ρ_2 , . . . , the total mass attenuation coefficient is given by

$$\frac{\mu}{\rho} = \frac{\mu_1}{\rho_1} w_1 + \frac{\mu_2}{\rho_2} w_2 + \cdots ,$$

where w_1, w_2 ... are the fractions by weight of the elements in the scintillator so that for high-energy gamma rays, the figure of merit of an absorber is given by

$$\frac{\mu}{\rho} \propto Z_1^2 w_1 + Z_2^2 w_2 + \cdots .$$

Thus, lower densities such as gases are used for the detection of low-energy X rays so that energy loss will occur within the detector rather than on the surface. Higher-density materials such as the heavy inorganic scintillators are used to detect the higher-energy gamma and cosmic rays.

In the case of scintillators the desired output is in the form of light. The process by which energy deposited in the material is transformed into light is a complicated one which is at best only partially understood. This conversion process is only partially complete so that a small percentage of the total energy lost is finally seen as light. Referring to this ratio as the scintillation conversion efficiency, we find that it varies for different phosphors.

For the sake of comparison, it is convenient to reference the light output of scintillator materials to that of thallium-activated sodium iodide, NaI(Tℓ), which has high quantum conversion efficiency relative to other materials (approximately 12 percent). Therefore, we shall state that a phosphor has a certain percentage of the light output of NaI(Tℓ).

The nature of the emitted light is another matter of concern. The wavelength must be compatible with the transmission properties of the scintillation material itself. The peak wavelength varies from the green to the ultraviolet region of the spectrum. Although the ultraviolet emission is not optimum, photomultiplier tubes with special glass or fused quartz windows which allow good light collection efficiencies at these wavelengths are available. The real difficulty comes from materials such as calcium fluoride (CaF_2), which has overlapping absorption and emission bands, thereby limiting the thickness of the scintillator.

Other important scintillation characteristics of phosphors are rise time and decay time of the light. These must be matched to the time constants of the photomultiplier tubes and counting circuits. In addition, they reflect the ability of the phosphor to act as a fast counter or to trigger other circuits. The rise times of only a few phosphors are well known and understood. In general, they have rise times on the order of a few nanoseconds and NaI(Tℓ), for example, has somewhat under 5 nsec of rise time. The decay times are better known and are tabulated in Table 1 in terms of microseconds.

The geometry of the high-energy experiments requires that large areas be exposed to the radiation flux to maximize the counting rates of the relatively diffused high-energy radiation. Furthermore, the necessity for screening out undesired background and spurious events requires the fabrication of elaborate collimators and guard crystals. Therefore, the mechanical characteristics of the material are very important. These are listed in Table 2.

One of the most important physical characteristics concerning the use of a material for scintillation counting is the available size. Some of the materials listed for consideration are available in small crystal sizes because of the cost of materials, difficulty in growing larger crystals, and, in some instances, the limitations imposed by the scintillation characteristics.

To be suitable for the instruments needed for the High Energy Astronomy Observatory (HEAO), the material must be machinable. It should also be resistant to the effects of moisture because working within a dry box imposes machining difficulties. The hygroscopicity is of less importance than it first

TABLE 1. SCINTILLATION PROPERTIES OF SCINTILLATION PHOSPHORS

	Scintillation[a] Conversion Efficiency (%)	Figure of Merit of Absorber ($\times 10^3$)	Maximum Scintillation Wavelength [nm (Å)]	Ultraviolet Cutoff Wavelength [nm(Å)]	Light Decay Constant (sec)	Comments
CaF_2(Eu)	50[b]	0.245	435 (4350)	405 (4050)	0.9	Moderate light output; self-absorption of scintillation light.
CsF	5	2.657	425 (4250)	220 (2200)	0.005	Very hygroscopic; very low light output; fast counting.
CsI(Na)	35	2.919	420 (4200)	260 (2600)	0.63	Good energy absorber; good light output; two modes of decay.
CsI(Tℓ)	45	2.919	565 (5650)	330 (3300)	1.0	Good energy absorber; fair-to-good light output
LiI(Eu)	35	2.664	470 (4700)	450 (4500)	0.94	Less efficient energy absorber; fair light output; self-absorption of scintillation light.
NaI(Tℓ)	100	2.397	410 (4100)	320 (3200)	0.25	Best light output; fair energy absorber.
TℓCℓ	1-2	5.634	460 (4600) 480 (4800)	390 (3900)	0.2	Very poor light output; best energy absorber.
Plastics	≈20[c]	≈0.050	350 (3500) to 450 (4500)	(d)		Fair light output for charged particles; not suitable for X ray; poor energy absorber; tends to have self light absorption problem.
Liquids	≈20[c]	≈0.050	350 (3500) 450 (4500)	(d)	0.002 to 0.008	Same as above.

a. Referenced to NaI(Tℓ)
b. 1.3 cm (0.5 in.) or less thick
c. Only true for charged particles, not X rays or gamma rays
d. Dependent upon composition

TABLE 2. PHYSICAL PARAMETERS OF SCINTILLATION PHOSPHORS

	Ease of Machining	Mechanical Characteristics (MOHS Hardness)[a]	Density (gm/cc)	Index of Refraction at Emission Maximum Wavelength	Solubility — Hot (gm/100 cc H_2O)	Solubility — Cold (gm/100 cc H_2O)	Hygroscopicity	Size Available, State of the Art[b] [cm(in.)]	Melting Point [°K(°C)]	Cost *Referenced* to a 7.6 x 7.6-cm Crystal[b]	Comments
CaF_2(Eu)	Easy by Grinding	Will Cleave Hard (4.1)	3.180	1.47	0.0017	0.0016	No	15.2 x 10.2 (6 x 4)	1633 (1360)	$ 2 088	Brittle; small sizes only; not toxic.
CsF	Difficult	Will Cleave Hard (2.4)	4.11	1.48	Very High	367	Very	7.6 x 7.6 (3 x 3)	1523 (1250)	$ 1 392	Difficult to fabricate; very hygroscopic; toxic.
CsI(Na)	Easy	Will Not Cleave Soft (1.8)	4.51	1.84	160	44	Slight	81.3 x 25.4 (32 x 10)	894 (621)	$ 1 218	Good mechanical characteristics; low toxicity.
CsI(Tℓ)	Easy	Will Not Cleave Soft (1.9)	4.51	1.80	160	44	No	81.3 x 25.4 (32 x 10)	894 (621)	$ 1 218	See above.
LiI(Eu)	Easy	Will Cleave Hard (2.4)	3.48	1.96	201	151	Very	20.3 x 15.2 (8 x 6)	719 (446)	$10 440	Very hygroscopic; poor mechanical characteristics; low toxicity.
NaI(Tℓ)	Easy	Will Cleave Moderately Hard (2.1)	3.66	1.85	302	184	Yes	81.3 x 25.4 (32 x 10)	923 (650)	$ 250	Hygroscopic; low toxicity; low cost.
TℓCℓ	Easy	Does Not Cleave Hard (2.5)	7.004	2.4	2.41	0.29	No	12.7 x 22.9 (5 x 9)	703 (430)	$17 400	Expensive; toxic (class B poison).
Plastics	Easy	Will Not Cleave Soft	1.06	Varies	Very Low	Very Low	No	Open	Varies	Varies	Good mechanically; not normally toxic.
Liquids	N/A	N/A	0.86	Varies	---	---	---	---	N/A	---	Problems in containment; toxicity varies.

a. MOHS scale: 1 for talc to 10 for diamond

b. Denotes cylindrical crystal diameter times length

appears because the material will be treated with considerable care and will be encapsulated for flight.

The toxicity of some compounds will complicate their machining and handling. Table 3 lists some toxicity considerations for phosphors.

DISCUSSION OF PARAMETERS USED IN TABLES

The following discussion clarifies the headings in Tables 1 and 2.

Table 1. Scintillation Properties

Scintillation Conversion Efficiency. When radiation traverses matter, some of its energy is dissipated into the material. By various mechanisms this absorbed energy is converted into light. The ratio of energy deposited in the crystal compared with the energy output as light is only 12 percent for NaI(Tℓ), which is the most efficient phosphor. Since NaI(Tℓ) has the highest efficiency, the other phosphors are compared with it as a standard.

Absorber Figure of Merit. For high-energy gamma radiation, the ability of a scintillator to absorb energy from the incident energy is proportional to the square of its electron density. Hence, the mass attenuation coefficient μ, in terms of density ρ, is proportional to Z^2.

Maximum Scintillation Wavelength (λ max.). The scintillation light is emitted in a nearly gaussian distribution, with peak emission at some wavelength which is designated at λ max. in Table 1.

As an example, NaI(Tℓ) has a photoemission peak at 420 nm (4200 Å) with one-sigma values approximately at 390 nm (3900 Å) and 450 nm (4500 Å). This is an easily usable spectral range and photomultipliers which match this are available.

Ultraviolet Cutoff Wavelength (λ co). This is the wavelength of radiation at which internal absorption becomes prohibitive. For some phosphors, it represents a limitation in the amount of internally emitted light that can be utilized.

Light Decay Constant. This is the length of time required for a light

TABLE 3. TOXICITY OF SCINTILLATION PHOSPHORS

	Degree of Toxicity and Subject Mammal
$CaF_2(Eu)$	None
CsF	0.5 g/kg of body weight — Man
CsI(Na)	1.4 g/kg of body weight — Mouse
CsI(Tℓ)	1.4 g/kg of body weight — Mouse
LiI(Eu)	1.1 g/kg of body weight — Mouse
NaI(Tℓ)	1.3 g/kg of body weight — Mouse
TℓCℓ	0.045 g/kg of body weight — Dog
Plastics	None
Liquids	Varies

pulse in the phosphor to decay to 1/e of the original value. It is expressed in microseconds and is indicative of the phosphors' usefulness for fast counting. The rise time for scintillation phosphors is difficult to actually measure and is known for only a few phosphors. It is usually on the order of nanoseconds and is somewhat less than 5 nsec for NaI(Tℓ).

A difference in decay time by almost a factor of four between NaI(Tℓ) and CsI(Tℓ) makes the phoswitch possible.

Table 2. Physical Parameters

Ease of Machining. This is a rather subjective parameter and is included only as a general comment. It should be realized that these are largely crystalline substances and machining them requires special tools, techniques, and experience. Figures 2, 3, and 4 indicate the results obtainable with the current state of the art.

Mechanical Characteristics. Some scintillator crystals will not cleave; that is, a crack will not propagate through the material. This is a desirable characteristic because cleavage is a property normally associated with brittleness. Hardness is stated first as relative to other phosphors and second in terms of the standard MOHS scale, which starts at 1 for talc and ranges to 10 for diamond.

Density. This is a useful parameter in that denser substances are usually better absorbers of energy. This is expressed in grams per cubic centimeter.

Index of Refraction. Index of refraction is a measure of a substance's ability to refract (or bend) light. A high index implies that light will be very much internally reflected and it will be difficult to optically bond light pipes or photomultipliers to it in such a way as to efficiently get the light out.

Solubility Hot and Cold. This parameter is measured in grams of substance which will dissolve in 100 cc of hot water (likewise in cold water). This is largely for information purposes as no HEAO applications will require water contact.

Hygroscopicity. This parameter is directly related to the two parameters just mentioned; however, it also includes surface effects and reactions with the dopant.

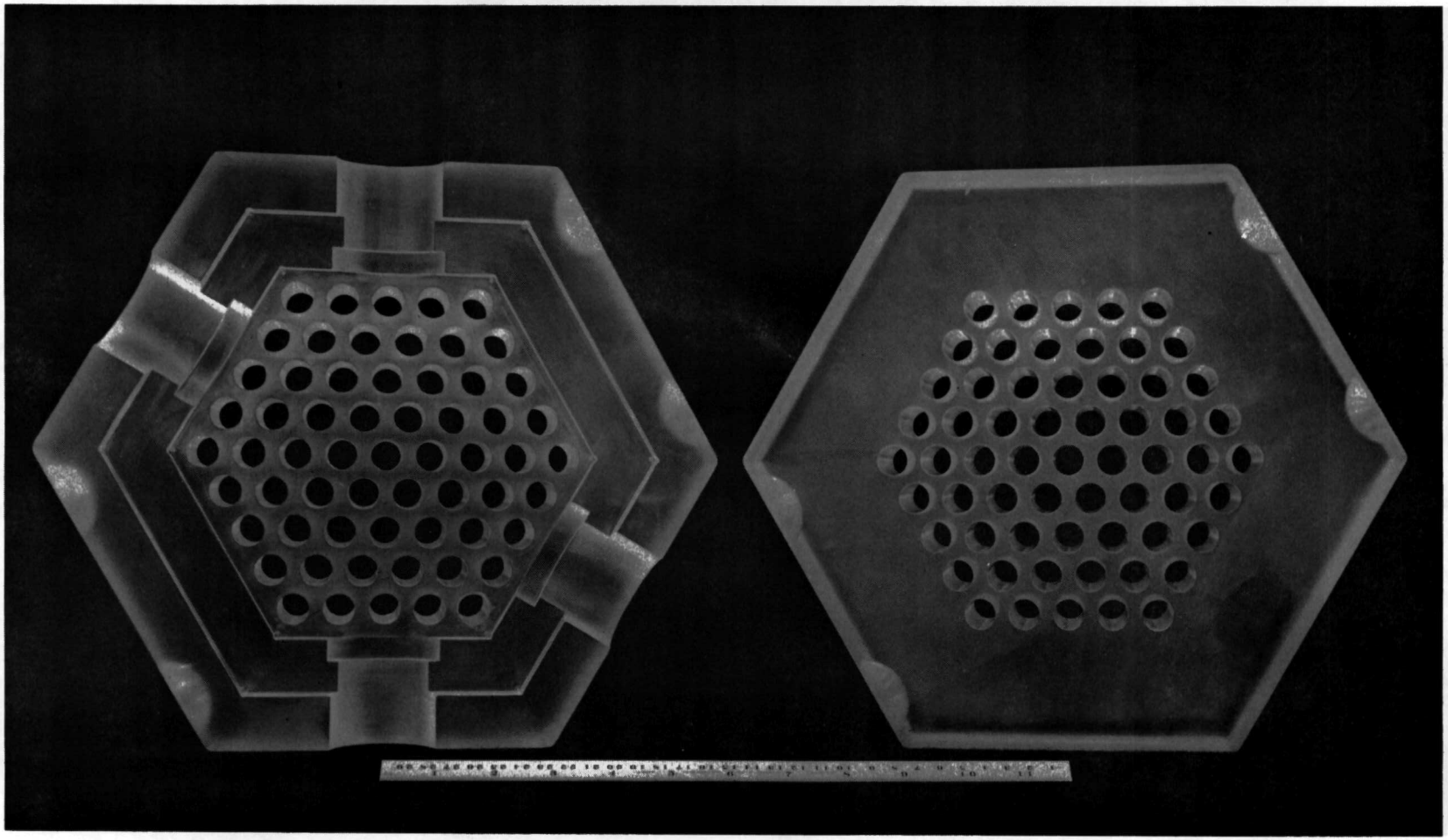

Figure 2. An example of machining which is achievable on cesium iodide by experienced craftsmen.

Figure 3. A finished 0.76-m (30-in.) sodium iodide detector before mounting and assembling.

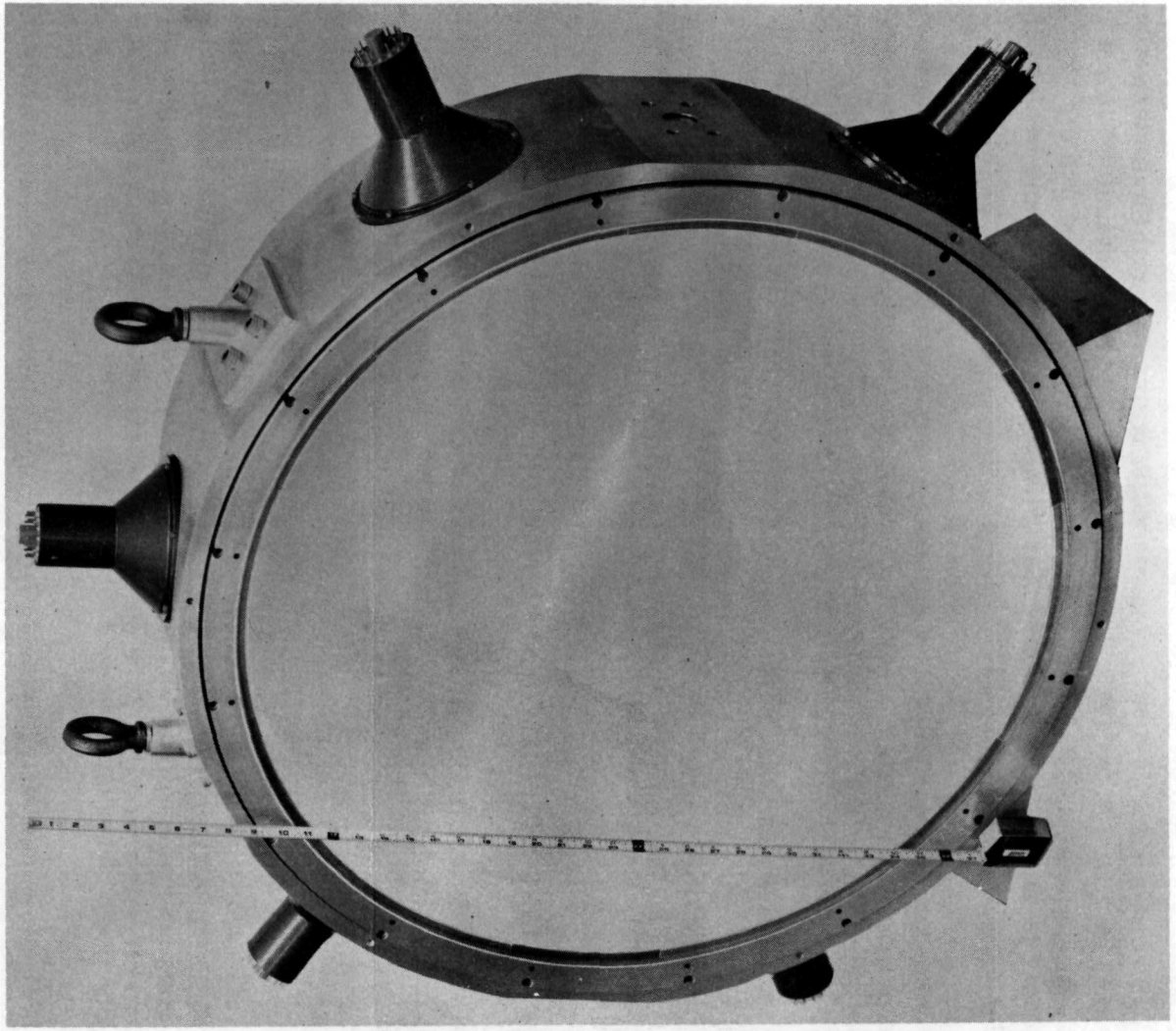

Figure 4. A mounted 0.76-m (30-in.) sodium iodide detector with photomultiplier tubes and handling fixtures installed.

In general, most of the phosphors will tolerate machining and assembly in humidity below 20 percent to 30 percent. All of the HEAO scintillators will be encapsulated during integration and will not be vulnerable to moisture after instrument fabrication.

Size Available. This is expressed in terms of a right cylinder, where 7.6 cm (3 in.) by 7.6 cm (3 in.), for example, implies a cylinder 7.6 cm (3 in.) in diameter and 7.6 cm (3 in.) high. The sizes quoted are for state-of-the-art techniques and do not necessarily represent what could be done if development work were to be conducted in the field of crystal growing.

Melting Point. This is expressed in degrees Kelvin and the figures serve primarily to reassure us that all phosphors mentioned would have no temperature limitation on the HEAO.

Cost. Cost is referenced to a 7.6-cm-by-7.6-cm (3-in.-by-3-in.) cylindrical crystal and represents state-of-the-art figures as of April 1971.

CHARACTERIZATION OF SCINTILLATION PHOSPHORS

Calcium Fluoride – Europium Doped – $CaF_2(Eu)$

This phosphor is well suited for charged-particle and low-energy gamma-ray counting; however, because of its low photoelectric attenuation coefficient, it has poorer energy resolution above a few hundred keV gamma excitation.

Its light output is fair and it has a maximum scintillation output in the blue. The doped form, however, has a self-absorption band which overlaps the emission band, diminishing the usable light for most applications. It has very good mechanical and thermal properties and has been used in oil-well logging. It will cleave but does possess good resistance to mechanical and thermal shock.

This phosphor has not been made in large quantities because of its self-absorption problem and its relatively high cost.

Cesium Fluoride – CsF

This phosphor has been used for special laboratory studies because of its extremely short decay constant. It is difficult to machine, extremely hygroscopic, and has been used only for specialized laboratory studies. The light output is very low and it is currently available only in small crystals.

Cesium Iodide – Sodium Doped – CsI(Na)

This phosphor has recently been perfected for applications requiring a high degree of mechanical and thermal ruggedness, while having a higher quantum conversion efficiency that the thallium-doped CsI. In almost all physical parameters, it is identical to CsI(Tℓ) and possesses its favorable characteristic of not cleaving and being relatively soft and machinable. As is true of most scintillation crystals, it requires certain special techniques and a good deal of experience to machine. However, from the standpoint of physical properties, the two forms of CsI are most desirable phosphors.

From the scintillation standpoint, CsI(Na) has the highest light output next to sodium iodide [NaI(Tℓ)]. The light output is comfortably into the blue region of the spectrum and there are no significant problems with self-absorption of the scintillation light. It has a higher mass attenuation coefficient than NaI(Tℓ); an example of this may be seen by observing the amount of CsI versus NaI necessary to absorb (1 - 1/e) of the total energy of a relativistic electron (Fig. 5). Only a 2-cm thickness of CsI is needed versus 5.7 cm of NaI.

The decay constant of CsI(Na) is not a simple exponential. The sodium-doped CsI is moderately hygroscopic but easily handled with simple precautions.

Cesium Iodide – Thallium Doped – CsI(Tl)

Most of the comments in the preceding section on sodium-doped cesium iodide apply here. Because CsI(Tℓ) was developed before CsI(Na), it has had more widespread use. Among its current uses are aboard spacecraft [such as the Orbiting Geophysical Observatory (OGO)] and in oil-well logging.

CsI(Tℓ) has a significantly shorter scintillation decay constant than NaI(Tℓ) and is commonly used in conjunction with it as a phoswich assembly[1]

1. Described in a later section titled Phoswich Description.

to exploit this different decay constant. The light output is lower than CsI(Na) but for certain applications its pulse shape characteristics make it preferable.

The crystal is not hygroscopic. The toxicity problem is of a very mild nature and, again, the most rudimentary precautions are satisfactory.

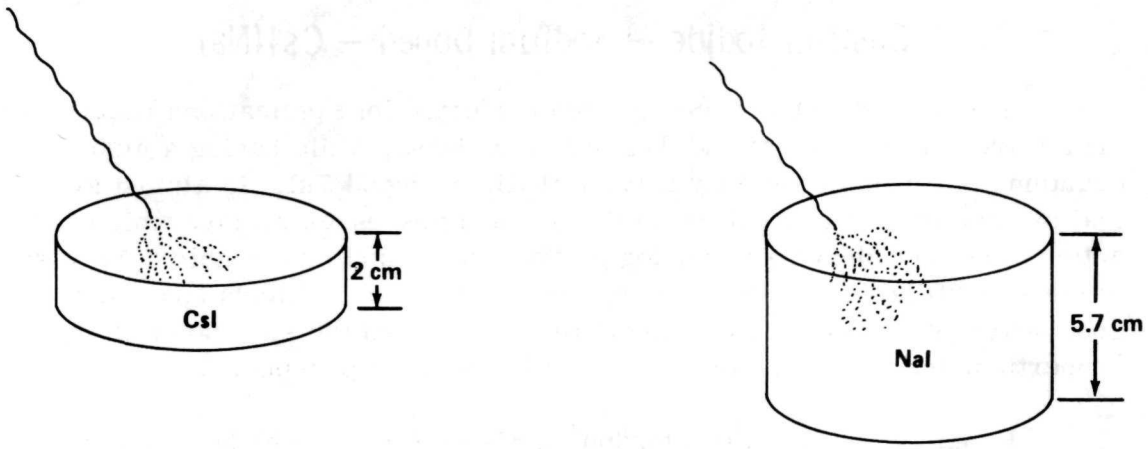

Figure 5. Equivalent radiation lengths for relativistic electrons in CsI and NaI.

Lithium Iodide – Europium Doped – LiI(Eu)

This phosphor is very useful as a neutron detector, particularly when the lithium is Li_6-enriched. However, it is a less efficient absorber of the higher-energy gamma and cosmic rays because of a lower ρZ^2 factor. It has only poor-to-fair light output, is available only in small ingot sizes, and is extremely expensive.

Sodium Iodide – Thallium Doped – NaI(Tl)

This is one of the earliest scintillation phosphors known and is probably the most commonly used, such as in many scientific instruments, laboratories, and for medical instrumentation.

As a scintillator it has a much higher efficiency than any of the others. Its conversion of energy lost, from radiation traversing it, into light approaches 12 percent.

As an absorber of energy it is not as effective as CsI or TlCl. It has a relatively fast scintillation decay constant, which makes it very useful combined with other phosphors in a phoswich configuration.

NaI is hygroscopic but can be readily machined and worked for all phases, except the final polishing or coating, in humidity up to 30 percent.

The relative toxicity is low and simple precautions seem adequate.

Thallium Chloride (TlCl)

This phosphor is highly expensive. It has a very high density and is the best absorber of all the existing scintillators. The light output is very low but it has a fast counting capability. Its present applicability is limited to the detection of high-energy gamma rays and charged particles in laboratories.

Plastic Scintillators

Plastic scintillators are of a wide variety but most share common characteristics. They have extremely fast counting times and are used for trigger scintillators and for time-of-flight measurements. They react well with charged particles but not well with gamma rays and are very useful as guard scintillators for high-energy gamma experiments. They machine easily and are relatively inexpensive. Their greatest handicap is that they have a very poor stopping power for gamma rays and cosmic rays and prohibitively large sizes would be required.

Liquid Scintillators

The preceding comments on plastics apply for the most part to liquid scintillators. In addition, however, there are special problems with liquid scintillators concerning containment bubble formation in zero g and the development of turbidity.

Polycrystalline Scintillators

A most recent development in the field of scintillators has been the fabrication of polycrystalline NaI(Tℓ), CsI(Na), and CsI(Tℓ). The scintillation characteristics of the polycrystalline versions are almost identical to the single crystal counterparts. The chief advantage provided by the polycrystalline material is the improvement in mechanical strength and in resistance to creep.

PHOSWICH DESCRIPTION

A phoswich is a unique kind of scintillation detector used to detect photons. Figure 6 illustrates a typical phoswich which is being used in the High Energy X-Ray Experiment (HEXRAY). This device has two scintillators with different rates of light impulse decay so that particle coincidences can be distinguished electronically with only one photomultiplier tube. These units perform three separate functions:

1. They exclude radiation which centers from an undesired direction. Such unwanted radiation will activate the CsI(Tℓ) scintillator. Because the decay constant of the CsI(Tℓ) scintillation process is relatively long compared with the NaI(Tℓ), sampling the light output at a given time after the control pulse will reveal which scintillators were activated. If at that time the light level exceeded some established value, the experiment's logic circuits will ignore that pulse.

2. They exclude radiation whose energy exceeds a certain value. In this experiment, photons possessing energy up to 150 keV will be completely absorbed by the 0.9-cm layer of NaI(Tℓ). If a more energetic photon is observed, it will pass into the CsI(Tℓ), where scintillation will occur. The resulting long tail on the light pulse will also cause rejection of the event.

3. They provide energy data on photons of interest. If no cancelling pulses are received from the CsI(Tℓ), the phoswich output pulse will be pulse-height analyzed. The amplitude of the photomultiplier output is then converted into digital form representing event energy for subsequent transmission or recording.

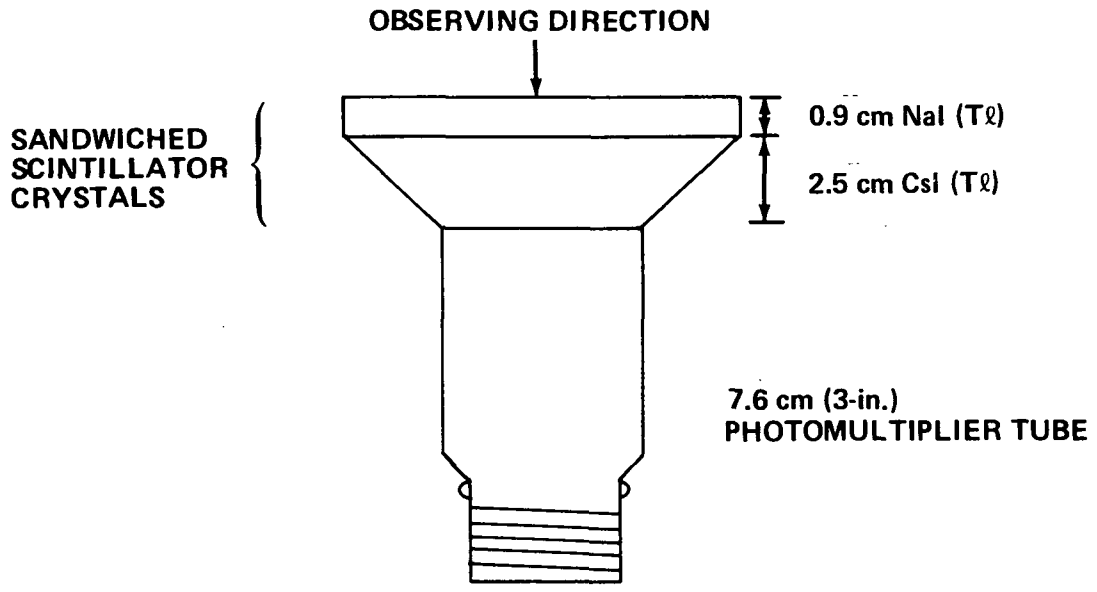

Figure 6. A typical phoswich.

TYPICAL SCINTILLATION DETECTORS

In a typical scintillation detector (Fig. 7), radiation (which can be from any direction) is converted into light and detected by the photomultiplier tube (PMT), which measures duration and intensity and produces a pulse whose magnitude is proportional to the incident energy.

Typical Scintillation Detector with Guard Crystal

In Figures 8 and 9, the typical detector of Figure 7 is surrounded by a crystal whose light is viewed separately. The crystals are optically decoupled and an electronic logic constraint is added so that any event which causes scintillation in both crystals is ignored. An event which causes scintillation only in the detector crystal is registered as a valid event. Therefore, only events entering through the acceptable angle (field of view) are registered by the system.

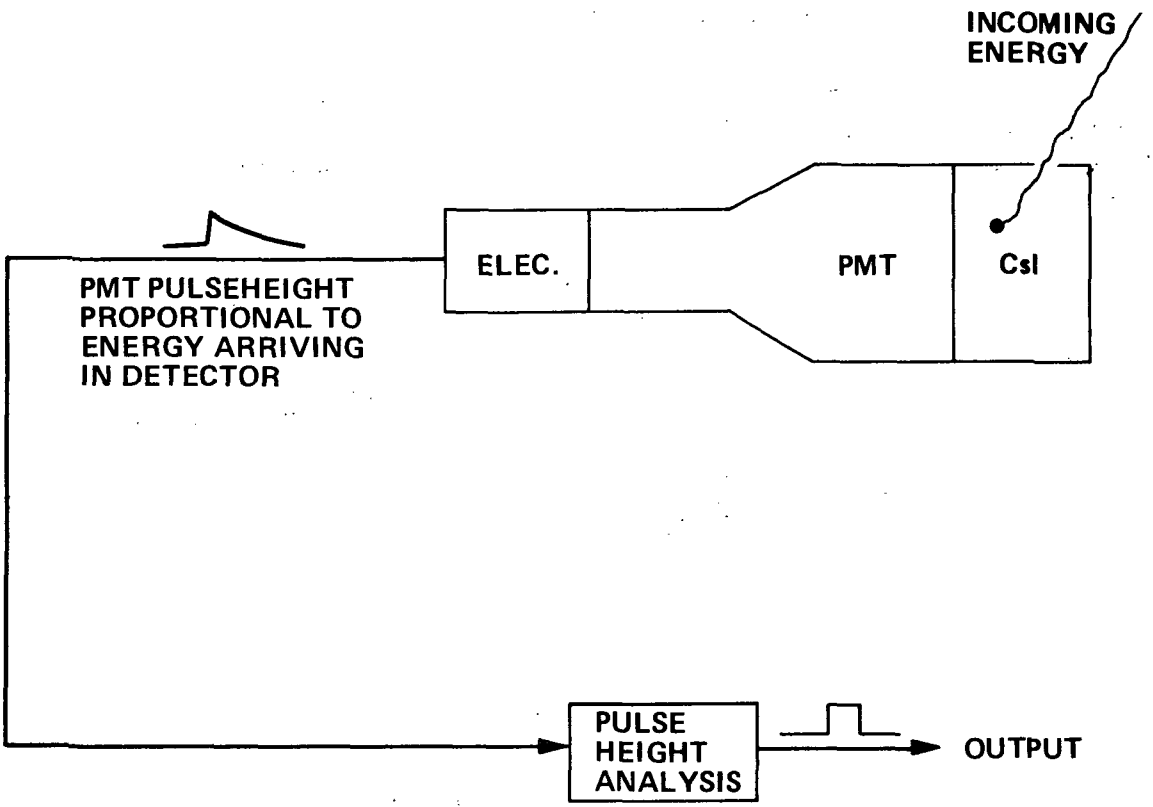

Figure 7. Typical scintillation detector configuration.

TYPICAL ORIGINAL HEAO-A EXPERIMENT INVOLVING CESIUM IODIDE

Figure 10 shows a typical configuration of an experiment involving cesium iodide which was to have been flown on the original HEAO-A. The configuration demonstrates the complex guard crystal geometry which is possible.

In Figure 10, six 7.6-cm(3-in.) phoswiches surround a central 12.7-cm(5-in.) phoswich. The guard scintillator is in the form of a central CsI crystal surrounded by six outer CsI pieces (all with photomultiplier tubes attached). Then a plastic guard scintillator is placed over the assembly to guard against charged particles which might enter as spurious events.

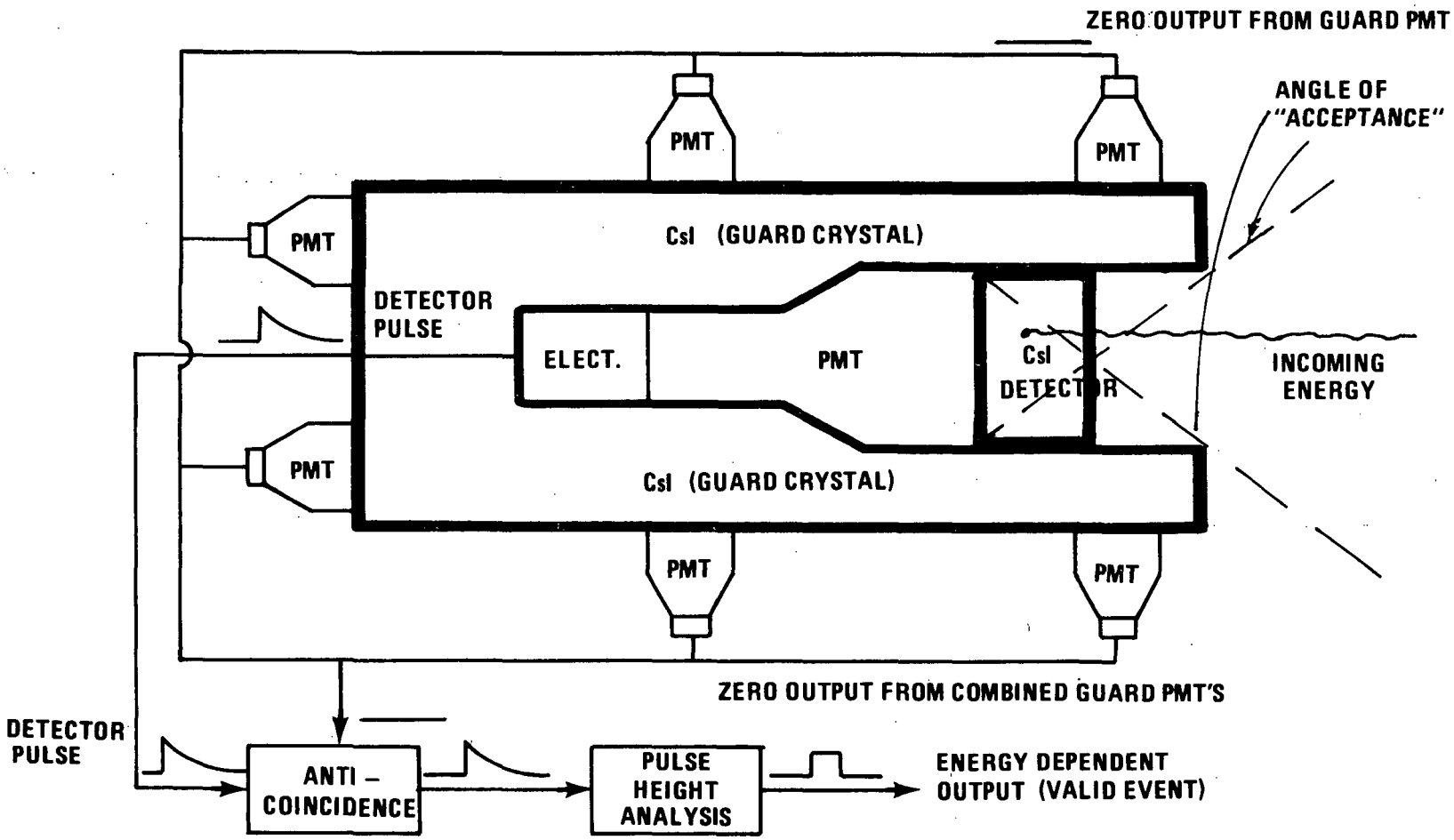

Figure 8. Typical cesium iodide detector and guard crystal — valid event registered.

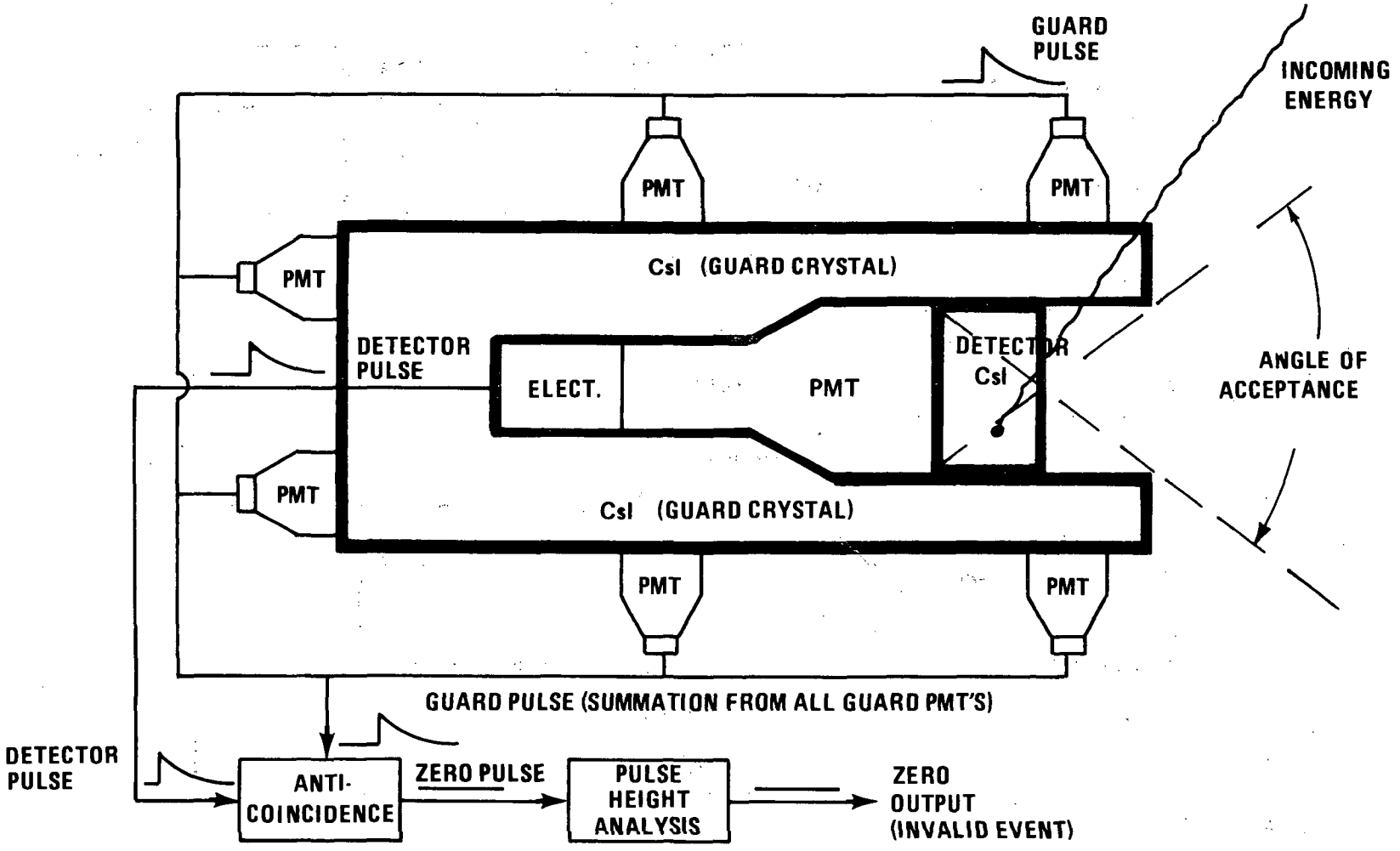

Figure 9. Typical cesium iodide detector and guard crystal — no valid event registered.

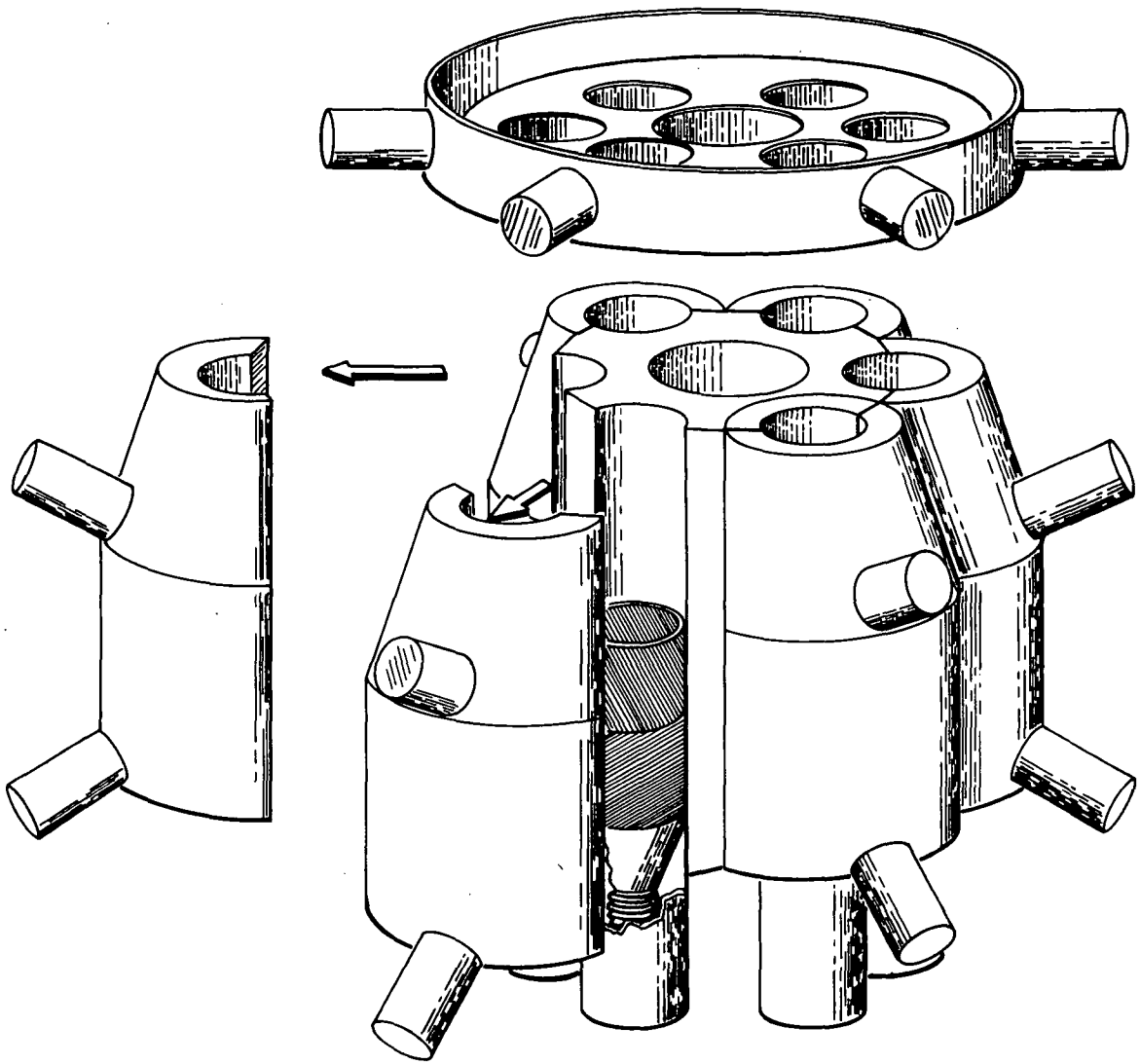

Figure 10. Typical exploded view of an MeV-range gamma-ray instrument for original HEAO-A.

PHYSICAL PROPERTY MEASUREMENTS[2]

The Materials Division of the Astronautics Laboratory at MSFC performed mechanical and thermal tests on cesium iodide doped with sodium and thallium. Although nominal values of the physical properties of undoped cesium iodide are available, systematic testing of doped cesium iodide has not been conducted previously.

All testing was performed in temperature-and humidity-controlled rooms at MSFC. Young's modulus, bulk modulus, shear modulus, and Poisson's ratio were obtained from ultrasonic measurements. Thermal expansion and thermal conductivity were temperature-dependent measurements which were made. The floating beam resonant technique and the ultrasonic velocity measurement technique were used to determine the elastic properties. The samples were physically tested by applying loads in tension and compression. An Instron Universal testing machine was used to apply the load at a constant rate of displacement.

The establishment of a reliable testing procedure for tension and compression measurements was complicated by the ductile nature of cesium iodide. Strain gages and a slow displacement under load were required to give the elastic portion of the stress/strain curve. The early measurements under tension did not give reliable Young's modulus values but the proportional limit and ultimate strength were obtained for a representative group of samples.

Thermal conductivity measurements at three different temperatures showed little variation for either CsI(Na) or CsI(Tℓ). The thermal expansion coefficient of both materials was determined with a quartz tube dilatometer. Measurements of the thermal expansion coefficient made at approximately 11° intervals, between 256°K and 422°K, were linear within ± 5 percent.

The compression test measurements are widely divergent. Their variation can be attributed to the crystalline character of CsI and the presence of

2. R. S. Snyder, G. E. Reynolds, and W. N. Clotfelter, Physical Property Measurements of Doped Cesium Iodide Crystals, Marshall Space Flight Center, to be published as a NASA Technical Memorandum.

grain boundaries, slip planes, and faults inherent in the grown crystal of large size. Although the variation in property values is not unexpected, the low proportional limit of some of the samples is a cause for concern. The variations are not attributable to either the sodium or thallium dopant, or to any specific region of the crystal.

Compressive creep measurements were started at MSFC in August 1972. These were measured with linear voltage differential transducers manufactured by the Daytronic Corporation. Rectangular samples of 1.6-cm^2 (0.25-square-in.) cross section areas were measured under a uniform loading using 13.6-kg weights. The tests were performed at normal room temperature and humidity conditions and precise temperatures were measured with thermocouples. The creep rate was measured several times a day as the ambient temperature changed. CsI(Na) showed slightly higher creep values than CsI(Tℓ).

The thermal expansion coefficient is large compared with most metals and must be an important consideration in the engineering design. The thallium-doped crystal had a consistent 10 percent higher thermal expansion coefficient than the sodium-doped crystal.

Although the average values of the mechanical and thermal properties are provided for experiment design, the wide variation in some of these values, caused by the crystalline and polycrystalline nature of the material, must be taken into consideration.

The following are the average values and the ranges of those properties measured:

1. Transverse Vibration

    a. Young's Modulus

        (1) Average — 1.6×10^{10} N/m^2 (2.4×10^6 psi).

        (2) Range - 1.6 to 1.8×10^{10} N/m^2 (2.3 to 2.6×10^6 psi).

2. Ultrasonic Velocity

    a. Bulk Modulus

        (1) Average — 1.21×10^{10} N/m^2 (1.75×10^6 psi).

        (2) Range — 1.10 to 1.35×10^{10} N/m^2 (1.60 to 1.96×10^6 psi).

b. Shear Modulus

(1) Average — 0.68×10^{10} N/m^2 (0.98×10^6 psi).

(2) Range — 0.62 to 0.793×10^{10} N/m^2 (0.90 to 1.15×10^6 psi).

3. Poisson's Ratio

a. Average — 0.26.

b. Range — 0.21 to 0.30.

4. Tension Tests

a. Proportional Limit [N/m^2 (psi)]

(1) Average — 1.86×10^6 (270).

(2) Range — 0.73 to 2.28×10^6 (106 to 330).

b. Ultimate Strength [N/m^2 (psi)].

(1) Average — 4.05×10^6 (588).

(2) Range — 2.24 to 11.86×10^6 (325 to 1720).

5. Compression Tests

a. Young's Modulus [N/m^2 (10^6 psi)]

(1) Average — 1.2×10^{10} (1.7)

(2) Range — 0.4 to 3.0×10^{10} (0.6 to 4.4).

b. Proportional Limit [N/m^2(psi)].

(1) Average — 1.12×10^6 (162).

(2) Range — 0.28 to 2.4×10^6 (40 to 341).

6. Thermal Measurements

a. Thermal Expansion

(1) CsI(Tℓ) — 5.4×10^{-5}/°K.

(2) CsI(Na) — 4.9×10^{-5}/° K.

b. Thermal Conductivity

(1) CsI(Tℓ) and CsI(Na) — 37×10^{-4} at 273° K and 323°K.

(2) CsI(Tℓ) and CsI(Na) — 39×10^{-4} at 373°K.

(See Fig. 11 for compressive creep.)

The following are the applicable formulas [1]:

$$\mu = V_T^2 \rho \quad ,$$

$$\sigma = \frac{1 - 2\left(\frac{V_T}{V_L}\right)^2}{2 - 2\left(\frac{V_T}{V_L}\right)^2} \quad ,$$

$$Y = 2\mu (\sigma + 1) \quad ,$$

$$K = \frac{Y}{3(1 - 2\sigma)} \quad ,$$

and

$$Y = 1.2615 \left(\frac{\rho L^4}{d^2}\right) F_T^2 \quad ,$$

where

μ = Shear modulus (N/m^2),

ρ = Density (kg/m^3),

V_T = Transverse velocity (m/sec),

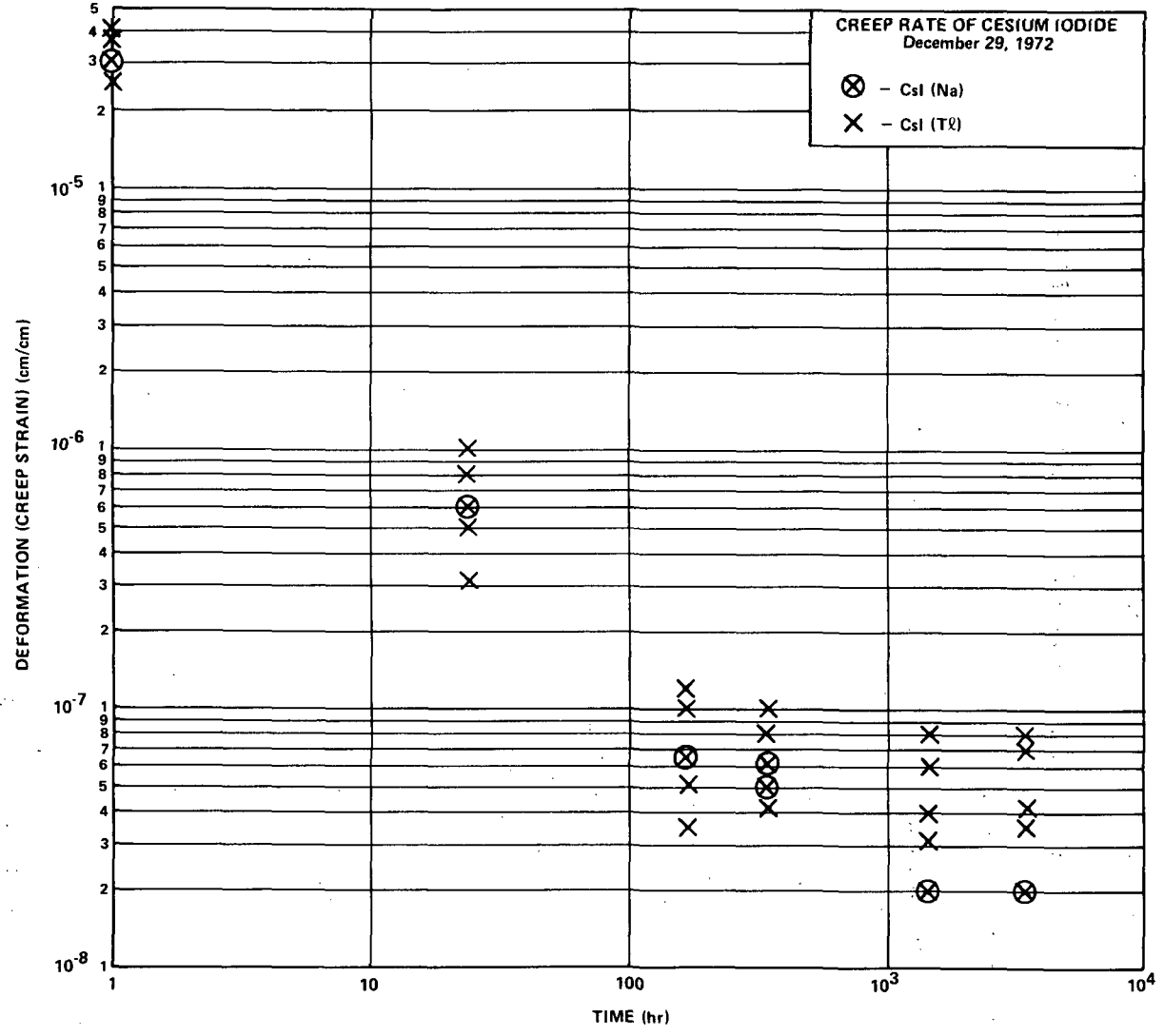

Figure 11. Compressive creep measurements.

σ = Poisson's ratio,

V_L = Longitudinal velocity (m/sec),

Y = Young's modulus (N/m^2),

L = Length (m),

d = Diameter (m),

F_T = Transverse resonant frequency,

and

K = Bulk modulus (N/m^2).

More details concerning aspects of the cesium iodide crystal technology are presented in Appendixes A, B, C, and D.

Page intentionally left blank

APPENDIX A
SCINTILLATOR PACKAGING

Prepared by

The Harshaw Chemical Company
Division of Kewanee Oil Company
Crystal & Electronic Products Dept.
Solon, Ohio 44139

for

National Aeronautics and Space Administration
George C. Marshall Space Flight Center
Marshall Space Flight Center, Alabama 35812

Under Contract NAS8-29032

Page intentionally left blank

APPENDIX A

SCINTILLATOR PACKAGING

Introduction

Crystal-phototube packaging techniques are important in the resolution, performance, and stability of scintillation detectors. The following must be considered in packaging: (1) the properties of the scintillator material involved (e.g., CsI is hygroscopic, dictating a hermetic container); (2) the type, number, and optical coupling medium required for the photomultiplier tube; and (3) efficient and uniform light collection transmission with the scintillation medium.

Scintillation Materials

The usefulness of a scintillation material as a radiation detector depends (1) on its ability to interact with radiation; (2) on its scintillation conversion efficiency (i.e., the fraction of incident energy absorbed which is converted to scintillation light) and (3) on the ability to remove and convey the scintillation to a light-sensitive device which produces an electrical signal. The device usually used is a photomultiplier tube.

A list of the physical properties for CsI(Na) and CsI(Tℓ) are given in Tables A-1 and A-2. The ability of CsI and NaI to interact with gamma radiation is given in terms of the linear absorption coefficient, T (cm^{-1}). The fraction of gamma photons absorbed is $f = (1-e^{-Tx})$, where x is the scintillator thickness. The linear absorption coefficient is given as a function of gamma-ray energy in Figures A-1 and A-2 for NaI and CsI respectively.

Also important is the time duration of the scintillation light output. The light output event is pulse-shaped with a "gradual" diminishing or decay of light output from peak value. Although the actual curve of light output versus time is not a simple mathematical function, the light output of NaI(Tℓ) can be approximated by a single component exponential decay of 0.250 μsec. Figure A-3 illustrates comparative decays for NaI(Tℓ), CsI(Na) and CsI(Tℓ), defining the longer decay times for CsI. The curves in Figure A-3 were developed by using a mathematical fit to three component exponentials for each material. Constants used for each exponential fit are given in Table A-1. Note the two-component fit for NaI(Tℓ), which gives a major component decay of 0.214 μsec.

TABLE A-1. PMT CURRENT OUTPUT VERSUS TIME FOR NaI(Tℓ), CsI(Tℓ), AND CsI(Na)

Exponential Coefficients and Time Constants	NaI(Tℓ)	CsI(Tℓ)	CsI(Na)
K_1	0.984	0.81	0.85
K_2	0.016	0.18	0.14
K_3	0	0.011	0.01
T_1	0.218 μsec	0.83 μsec	0.41 μsec
T_2	1.34 μsec	4.65 μsec	2.56 μsec
T_3	—	25.8 μsec	30 μsec
K_1T_1	0.214 μsec (91%)	0.672 μsec (37.6%)	0.35 μsec (34.7%)
K_2T_2	0.021 μsec (9%)	0.835 μsec (46.5%)	0.358 μsec (35.5%)
K_3T_3	0 (0%)	0.284 μsec (15.9%)	0.30 μsec (29.8%)
$K_1T_1 + K_2T_2 + K_3T_3$	0.235 μsec (100%)	1.791 μsec (100%)	1.008 μsec (100%)

Light output as a function of time for CsI(Na) and CsI(Tℓ) is more complicated but can be approximated by single-component exponential of 1.1 μsec and 0.8 μsec, respectively. The time dependence of light output for these scintillators depends on the dopant concentration and temperature. The relative light output of NaI(Tℓ) (as a function of dopant concentration) is illustrated in Figure A-4. The relative light output of NaI(Tℓ), CsI(Tℓ), and CsI(Na) are illustrated in Figure A-5 as functions of temperature. Also illustrated is the CsI(Na) linear response over the normally encountered temperature range (to ~ 333°K) allowing simple electronic pulse height compensation.

Optical Considerations of Scintillation Detectors

The purpose of light-coupling optics and, to some degree, the crystal geometry itself, is to direct as much scintillation light as possible to the

TABLE A-2. EFFECT OF SURFACE FINISH AND REFLECTOR ON CRYSTAL PERFORMANCE

	Surface Preparation and Crystal Mounting	Pulse Resolution (%)	Pulse Height (V)
A	Solvent polished	16.6	29.0
B	Back and side roughened with 80-grit emery paper	13.0	36.0
C	Solvent polished and surrounded by MgO powder	13.8	33.8
D	Back and side roughened with 80-grit emery paper and surrounded by MgO powder	12.2	40.8
E	Back and side roughened with 80-grit emery paper and given a hydrate coating	12.5	37.1
F	All surfaces roughened with 80-grit emery paper	13.1	34.2
G	Back and side mechanically polished with 4/0 emery paper	16.3	30.8
H	Back and side roughened with 80-grit emery paper and coated with TiO_2 pigment	15.3	30.0
I	Back and side roughened with 80-grit emery paper and covered with aluminum foil	13.0	36.0

photocathode of the photomultiplier tube. This must be done, however, in such a way that the response to scintillation does not depend on the region of the scintillator in which the scintillation occurred. These two requirements

Sample	Remarks on Surface Quality	Optical Path (cm)	T(635 nm) %	T(425 nm) %	$\frac{T_{red}}{T_{blue}}$	$\frac{T\ (encap.)}{T\ (unencap.)}$ 635 nm	$\frac{T\ (encap.)}{T\ (unencap.)}$ 425 nm
CsI(Tℓ) Single Crystal (Arlene's)	First Polish — Poor		58	39	1.5		
	Second Polish — Good	2.7	63	51	1.23		
	Second Polish — Encapsulated		81	75	1.08	1.3	1.47
CsI(Na, Tℓ) Polyscin $2 \times 4 \times 5$ cm^3 Sample No. 1	As Received						
	Good	5	62	50	1.24		
	Poor	4	43	32	1.35		
	Poor	2	46	35	1.31		
	Encapsulated:						
	Good	5	74.5	64	1.16	1.2	1.28
	Poor	2	68	60	1.14	1.47	1.70
CsI(Na, Tℓ) Polyscin $2 \times 4 \times 5$ cm Sample No. 2	As Received						
	Not So Good	5	51	38.5	1.32		
	Poor	4	37	27.5	1.34		
	Not So Good	2	53	42	1.25		
CsI(Na) Single Crystal 2.5×2 cm	Well - Polished; Not As Clear As CsI(Tℓ), Single Crystal Sample (Arlene's)	2	68.5	53	1.3		
CsI(Na) Polyscin 4.5×6.4 cm Sample No. 3	As Received						
	Fair	6.4	49	41	1.2	1.55	1.70
	Encapsulated		76	70	1.08		

Figure A-1. Complete cross sections of cesium iodide illustrating total absorption and fractional components due to Compton absorption, photoelectric absorption, and pair production.

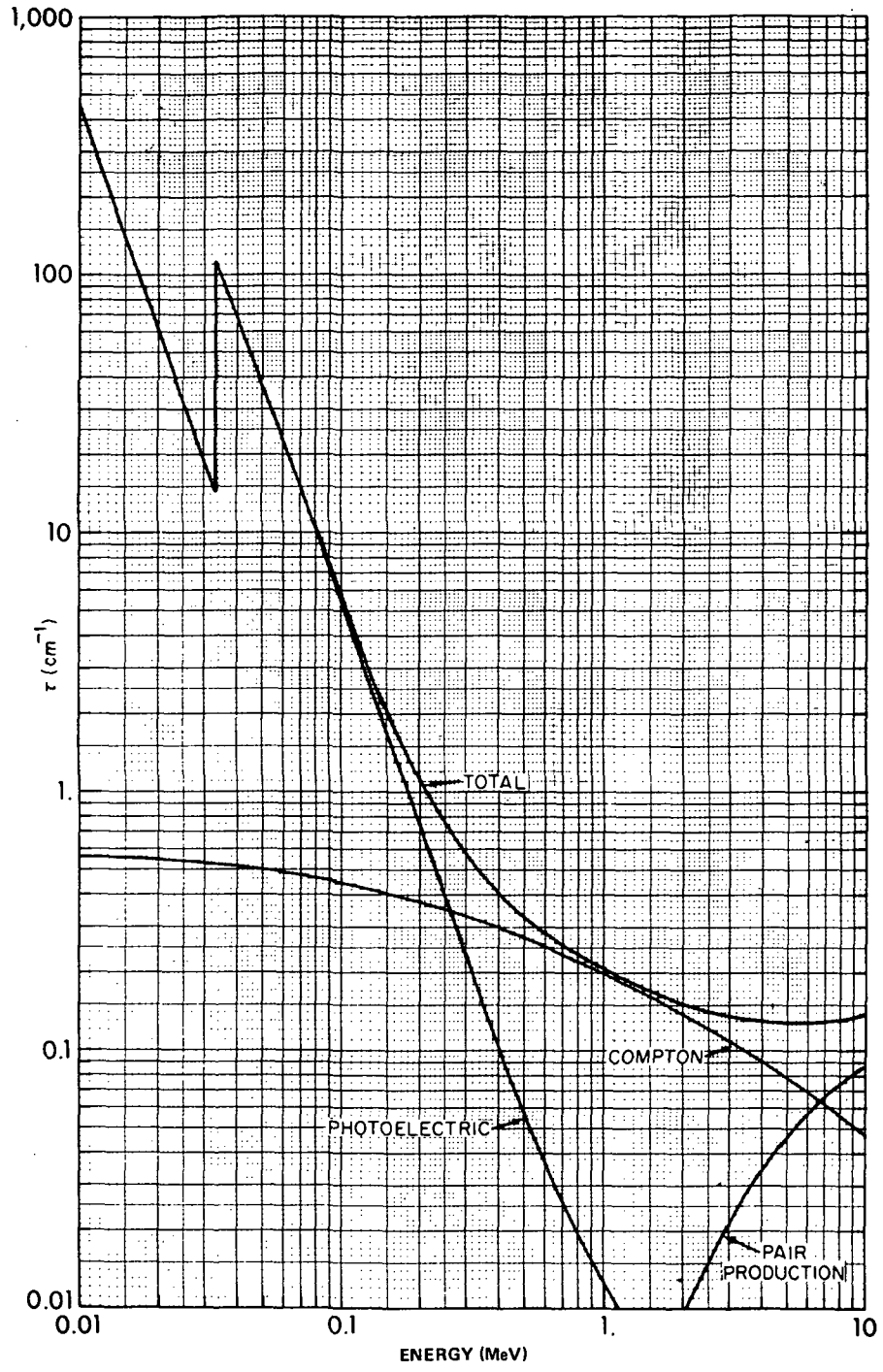

Figure A-2. Complete cross sections of sodium iodide illustrating total absorption and fractional components due to Compton absorption, photoelectric absorption, and pair production. (Curve ratios have been corrected for coherent scattering.)

conflict, in general, but the degree to which they are met will determine the energy resolution obtainable with a given detector.

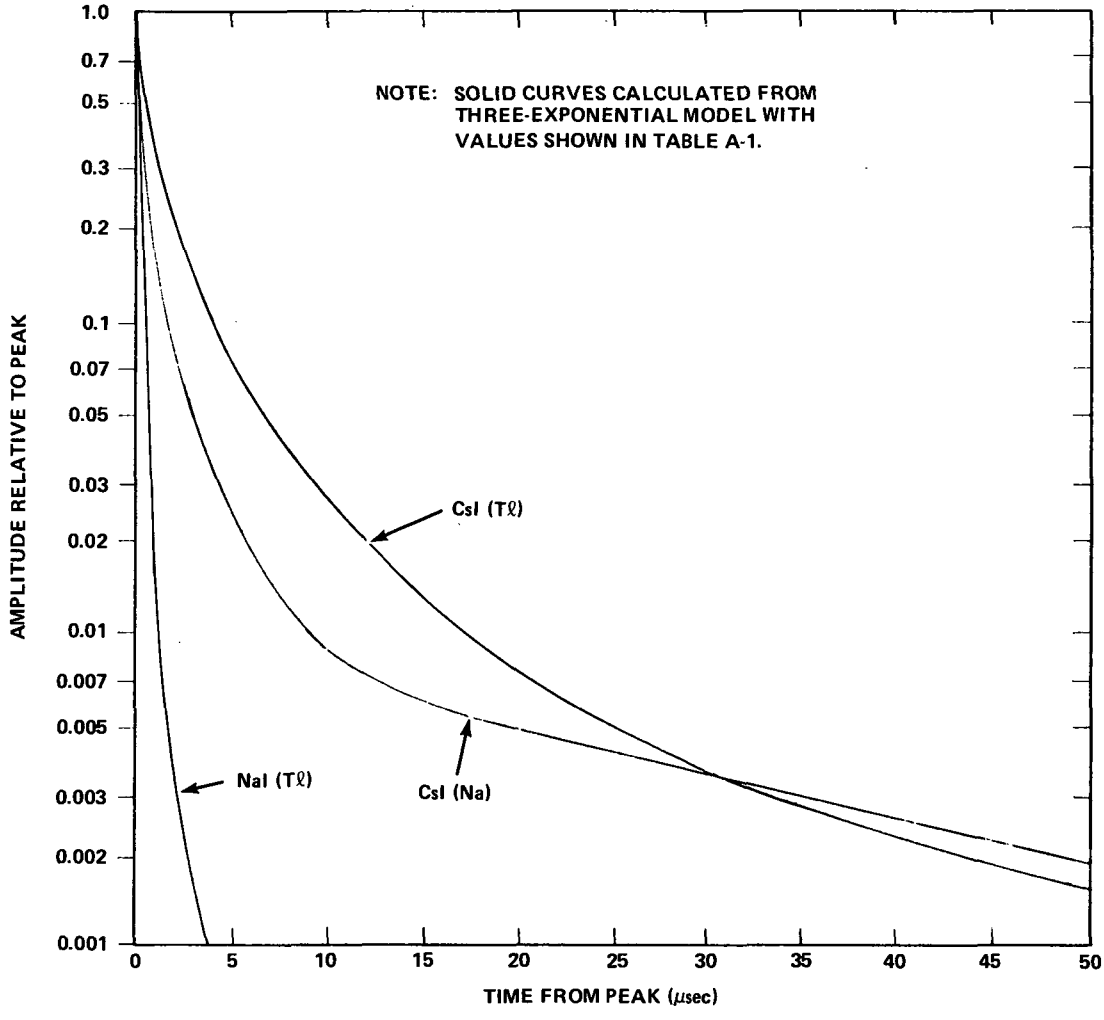

Figure A-3. PMT current decay from NaI(Tℓ), CsI(Tℓ), and CsI(Na) at 293°K.

The resolution of a gamma ray scintillator spectrometer is its ability to display as separate peaks in the output spectrum two gamma rays whose energy differential is small: The ideal gamma ray scintillation spectrometer would yield a single line of zero width in the output spectrum for monoenergetic incident gamma rays. However, in actuality, spectrometers have an instrumental line width to contend with, which limits the resolving power (the ability to separate closely spaced lines) of the spectrometer.

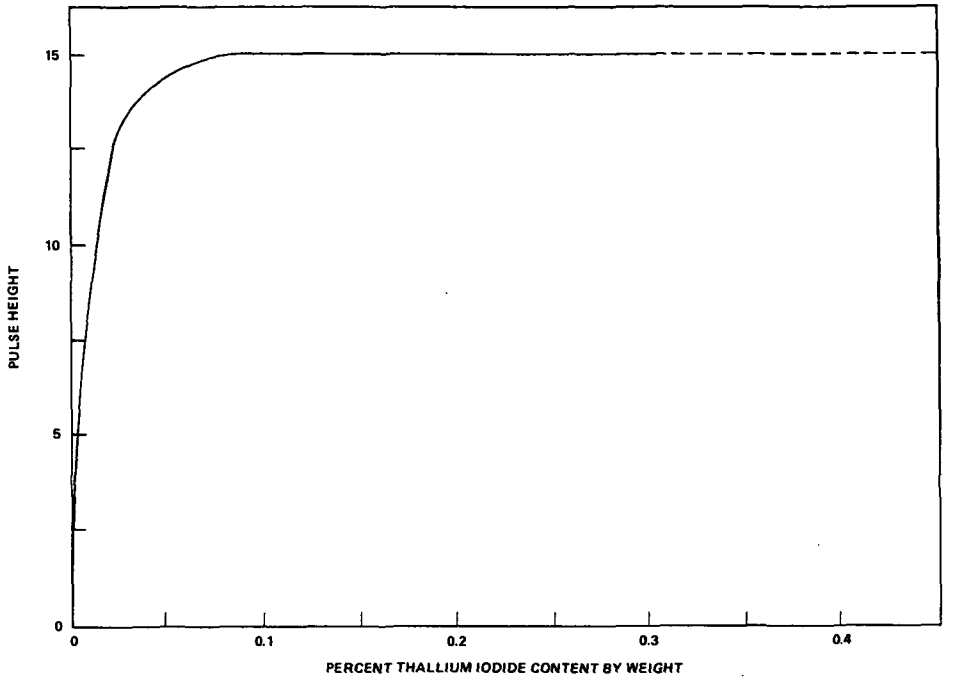

Figure A-4. Effect of thallium content on pulse height of the Cs^{137} photoelectric peak recorded by 1.3-cm (0.5-in.)-thick, 2.5-cm (1-in.)-diameter NaI(Tℓ) crystals.

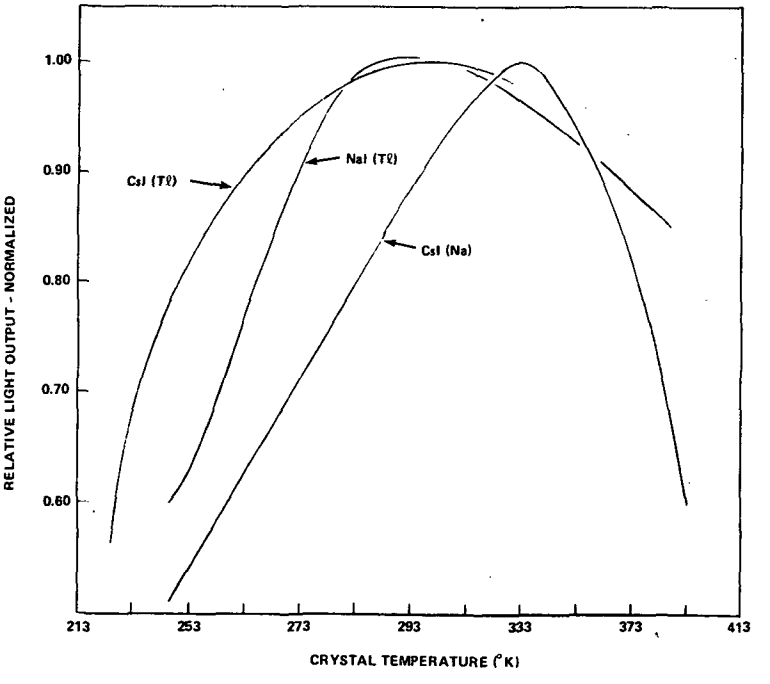

Figure A-5. Relative light output of NaI(Tℓ), CsI(Na), and CsI(Tℓ) as a function of temperature.

Instrumental line width in gamma ray scintillation spectrometers is due to several factors: (1) variation in light collection efficiency throughout the volume of the scintillation crystal, (2) variations in energy conversion efficiency throughout the volume of the crystal, and (3) nonuniformity of the photocathode viewing scintillation events in the crystal. Factor (1) is a significant variable as far as most practical crystals are concerned. Factor (2) is small compared with factor (1) in the case of a good quality scintillation crystal. However, in low-grade material it can become the dominant factor. Factor (3) is only important when scintillations are occurring near the photocathode. Factors can be independently measured but in an assembled detector only their combined effect is measured. What one observes is a variation in output pulse height as a point source of γ-radiation moves over the surface area of the crystal. For most cases of interest, the dominant factor being so measured is factor (1). Thus, these variations mean that some regions of the crystal are giving higher light output than others. It should be noted that if a reduction of light output in the crystal where light output is high were possible, and also if an increase in the light output in regions of the crystal where light output is low could be obtained, the total effect would be that every region of the crystal would give rise to the same light output. Such a balanced light output would result in minimizing the effects of factors (1), (2), and (3). A reduction of variations in these foregoing factors will result in a reduction of the instrumental line width.

A compensating technique makes it possible to reduce the light output in regions of the scintillator in which it is high and to increase the light output in regions where it is low. The compensation is obtained by allowing the reflectance of the scintillator surface to vary. This will be discussed further under the heading, Crystal Surface Finish.

For CsI at high energies (above 2 MeV), uniformity of light collection is by far the more important factor to be optimized whereas in the X-ray region (100 keV and below), maximum light collection and quantum efficiency of the photomultiplier are of the most importance. This is because of the statistical nature of scintillation photon production. Uniformity problems in a detector designed for the X-ray region are usually mitigated by the smaller detector sizes needed.

Some important considerations in the optimization of the energy resolution of the detector are discussed in the following subsections.

Refractive Index of the Crystal. To detect the scintillations which occur within the crystal, the light must be transmitted from the crystal to the

photomultiplier tube. Consider a light beam traveling from a medium of index of refraction n_1 into a medium of index of refraction n_2, where $n_1 > n_2$ (Fig. A-6). If θ_1 is the angle of incidence and θ_2 is the angle of refraction, then

$$n_1 \sin \theta_1 = n_2 \sin \theta_2 \quad .$$

For some values of n_1, n_2, and θ_1, θ_2 can be equal to 90 deg. This means that the amount of transmitted light is zero, or total internal reflection occurs. With $\theta_2 = 90$ deg, the preceding equation becomes

$$\sin \theta_2 = \frac{n_2}{n_1} \quad ,$$

where θ_2 is defined as the critical angle at which total internal reflection occurs. For angles of greater than θ_2, the incident light is totally reflected back into medium 1.

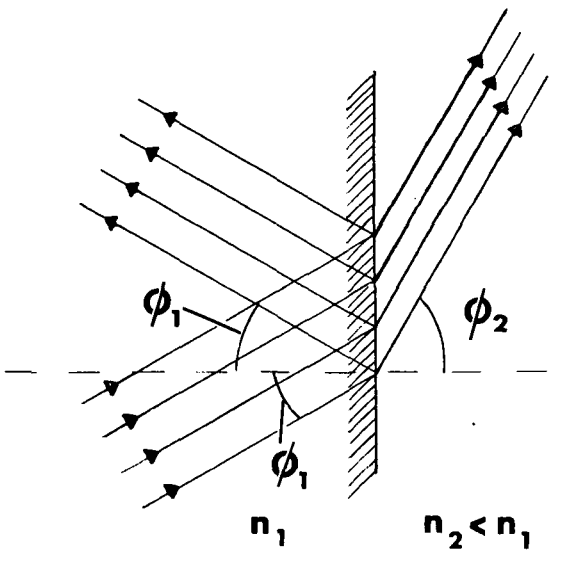

Figure A-6. Refraction and reflection at optical boundary.

Alkali halides considered here have relatively high indices of refraction (~ 1.8) at their emission wavelengths. For a crystal-air interface (the index of refraction of air is approximately 1.0), θ_2 is 34 deg. Thus any light incident at angles greater than 34 deg will not escape the crystal but will be totally internally reflected. For a crystal-glass interface (the index of glass is approximately 1.5), θ_2 is 54 deg.

Even at normal incidence some light is reflected. The fraction reflected is given by $R = (n_1 - n_2)^2/(n_1 + n_2)$, where n_1 and n_2 are the respective indices. For a crystal-air interface $R \simeq 1.5$ percent. Furthermore, the reflection coefficient increases rapidly as the critical angle is approached.

In practice, scintillation crystals are joined to the glass faces of photomultiplier tubes by interface fluids such as silicone greases (index ~ 1.5). This eliminates air spaces which would decrease the amount of light transmitted

to the photomultiplier tube. In addition, the surface of the crystal is treated and reflective materials are used on the outside of the crystal and the photomultiplier envelope to reduce the loss of light from the crystal at surfaces other than at the photomultiplier tube interface (Fig. A-7). Because of reflections at crystal-air interfaces, open cracks which may appear in the crystal may affect the performance as a detector. The effect, if any, depends on the size, direction and location of the crack(s).

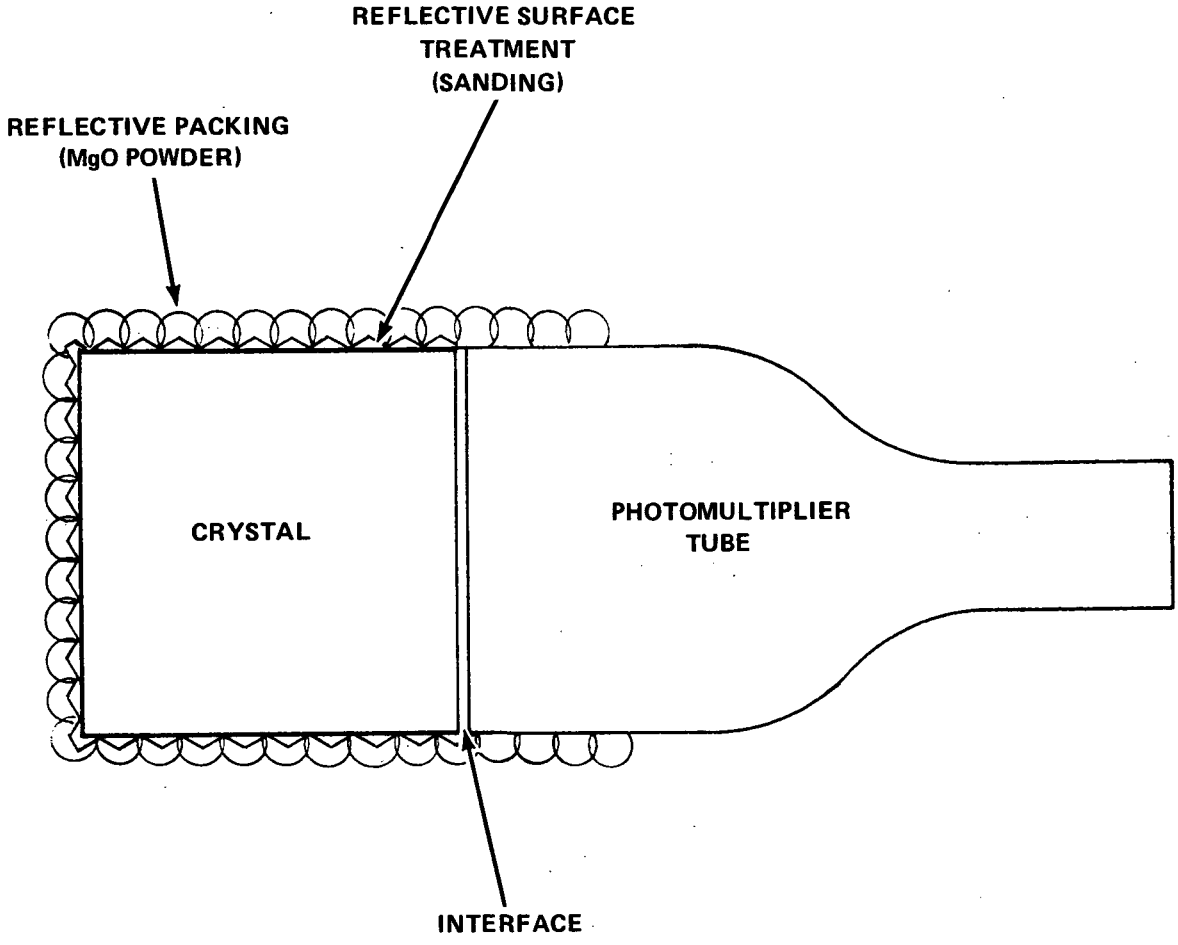

Figure A-7. Scintillation detector reflective details.

Crystal Surface Finish. In a typical detector only a modest fraction of the scintillation light reaches the photocathode of the photomultiplier tube directly. The remainder of the light may reach the photocathode after one or

more scatterings from the sides of the crystal or from the housing in which the crystal is contained. The surface of the crystal can be treated to enhance the scattering of light back into the crystal. As a general rule, NaI performs better if it is abraded by sanding, whereas CsI performs best when completely polished (this can be determined only by actual trial in the particular geometry). Apparently for NaI(Tℓ) the sanding process creates tiny fractures and irregular cleavage surfaces which cause high reflectivity by virtue of total internal reflection.

Reflective coatings may be divided into two broad classes — diffuse reflective coatings and specular reflective coatings. A diffuse reflective coating will reflect a beam of light in all directions. A specular reflective coating will reflect a beam of light unidirectionally. Diffuse coatings are metal oxides such as magnesium oxide and aluminum oxide while specular reflective coatings are mirror-finish metallic coatings such as mirror aluminum and silver coatings. In most scintillator applications diffuse reflectors are used either as coatings or as packing material around the scintillation crystal.

Studies of scintillator surface preparation versus performance have been published for NaI(Tℓ). Table A-2 illustrates the results of a study by Harshaw Chemical Company. The NaI(Tℓ) crystals were tested with different types of reflectors in combination with the different surface finishes.

The tests were conducted by placing the various surface finishes on thallium-activated sodium iodide crystals which are 2.5 cm. (1 in.) in diameter by 1.3 cm (0.5 in.) thick. The evaluation of the crystals was based on the criteria of pulse height and pulse resolution. The pulse height and pulse resolution are measurements (at the 661 keV Cs^{137} photo peak) made with a pulse height analyzer. The surface finish-reflector combinations tried are listed in Table A-2. For A, B, F, and G the aluminum crystal housing acted as a reflector, while for C, D, E, H, and I, the auxiliary reflector listed for each in Table A-2 was used. A solvent-polished surface was prepared with an acetone-chloroform treatment. In all cases but F the crystal face was solvent-polished before being joined to the glass window with an optical coupling agent such as a silicone grease, while for F the crystal was roughened before it was coupled with a silicone grease. A hydrate coating (which gives a white opaque surface) was prepared by wetting the crystal with water and heating it under vacuum for several hours. TiO_2 pigment used in case H was composed of TiO_2 powder suspended in a thermosetting plastic.

Poor pulse resolution measured in all cases is not due to substandard crystals but to poor optical coupling supplied by the light pipe and to the non-uniform photocathode used. However, the poor resolution should not invalidate

the comparisons made between the different methods of preparation. Two crystals were used for these tests since several of the surface preparations are destructive. The two crystals were first compared after having been mechanically polished with 4/0 emery paper. They gave identical pulse heights and pulse resolutions.

The results in Table A-2 show the superiority of roughened crystals over solvent-polished crystals. Improvement in light collection of the roughened crystals is caused by the roughened surface diffusing the incident light and cutting down on light trapped within the crystal by specular reflections. The surface resulting from mechanical polishing with 4/0 emery paper, case G, is hardly better than the solvent-polished surface, probably because the surface produced by this fine abrasive is too smooth to create any appreciable diffusion of the light from scintillations.

Reflectors, as expected, performed in accordance with their reflecting efficiency, the best being MgO powder and the hydrate coating. This coating turns yellow with time and is initially yellow for crystals with high thallium contents; therefore, it is not a practical surface finish. The TiO_2 has an ultraviolet absorption which accounts for its relatively poor performance.

Bright-dipped aluminum is an efficient reflector but is not quite as good as MgO. $A\ell_2O_3$, although not shown in the table, was found to be similar to MgO.

Reflectivity of Crystal Packaging. Even with optimum surface treatment, a significant amount of light can escape the crystal. This can be minimized by surrounding the crystal with a highly reflecting material such as MgO or $A\ell_2O_3$ in powder form. The powder is packed firmly around the scintillator with appropriate spacers and retainers.

White paints in general are not as good. They have about a 90 percent reflectivity compared with the best available $A\ell_2O_3$, which has 98 percent reflectivity. Because the paint has an index considerably above that of air, the paint on the crystal surface mitigates in part the production of optimum crystal surface finish.

Crystal Geometry. Experience has shown that a crystal in the form of a right circular cylinder whose length is approximately equal to its diameter gives the best performance when viewed by a photomultiplier on the circular face. Whenever this geometry is changed, performance will suffer unless great care is taken in the placement of phototubes. Long, narrow geometries, recesses, projections, etc., should be avoided because they inhibit uniform light collection.

Quantum Efficiency of Photomultiplier. Photomultiplier tubes available today are improved greatly over earlier tubes, but quantum efficiencies are still only approximately 25 percent and may vary by a factor of three to one over the photocathode area. By using a light pipe between the crystal and the photomultiplier, scintillation light is more uniformly spread over the photocathode area. The emission spectra of NaI(Tℓ), CsI(Na), and CsI(Tℓ) are shown in Figure A-8. To obtain the maximum sensitivity, the S-11 photocathode is usually used because the spectral response of this tube accommodates the emission spectra of aforementioned scintillators.

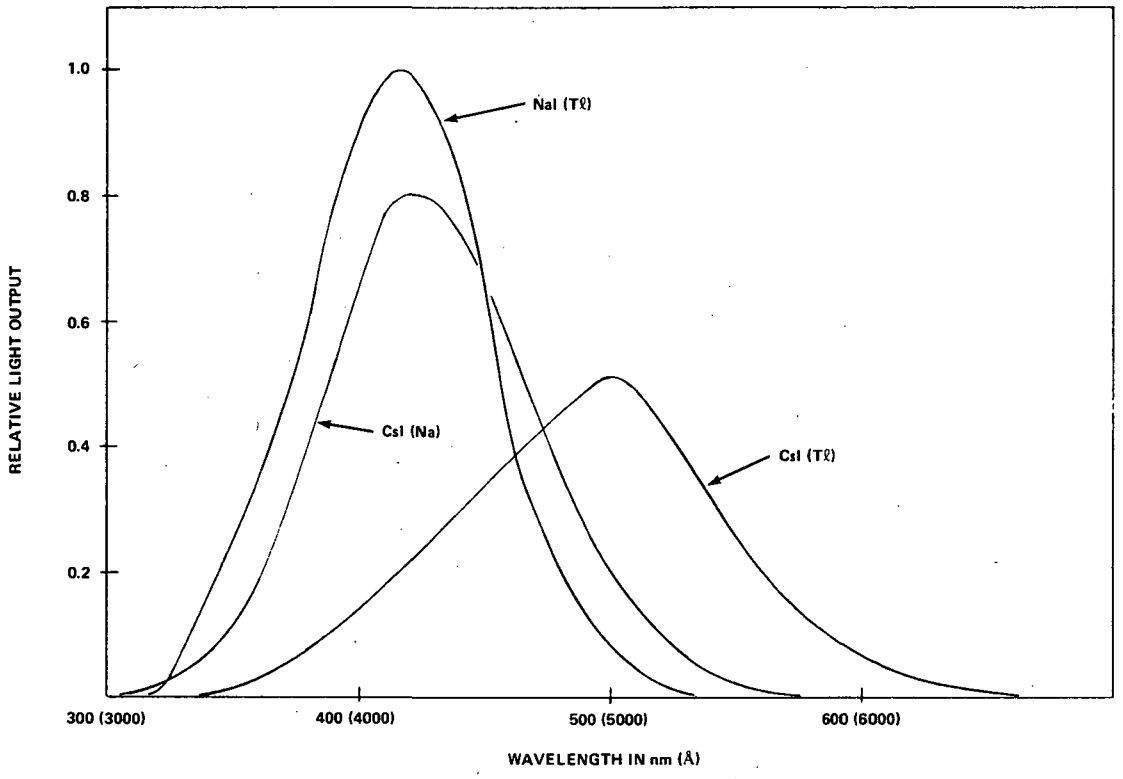

Figure A-8. Emission spectra of NaI(Tℓ), CsI(Na), and CsI(Tℓ).

Number and Position of Photomultiplier Tubes. In general, the larger the photocathode the better the light collection efficiency. For optimum resolution, the greatest amount of cathode area physically possible should view the light output of the crystal. Therefore, tubes on both ends of a large crystal will improve the resolution. When using multitube units, care must be

given to selecting a photomultiplier with high quantum efficiency and good stability. The gain of each photomultiplier or photomultiplier crystals must be carefully adjusted so that each tube has the same pulse height output at all times. Phototubes generally having a "venetian-blind" dynode structure are used when timing response is not the prime consideration but good stability and resolution are needed. When time response is the prime consideration, a phototube with a smaller cathode area and faster timing response is satisfactory.

Photocathode uniformity becomes much more important when thin scintillators are used. Photocathode uniformity is important as the energy of the incident radiation decreases and the number of photons per disintegration is reduced.

Photomultipliers with 12.7-cm (5-in.) diameter photocathodes are the largest size recommended for use in scintillation detectors because the cathode nonuniformity of the larger tubes is greater.

Optical Transmission of Coupling Medium. When it is necessary to separate the photomultiplier tube from the crystal, windows are provided for viewing the light from the encapsulated crystal. The optical glass windows (and light pipes) used on scintillation detectors clearly must have high transmission to the scintillation emission spectra. For the scintillation considered here, considerable light is emitted even at 390 nm (3900 Å). Pyrex glass and most epoxy coupling compounds have absorptions which begin in this region and extend into the ultraviolet, and therefore care must be taken in their use. Quartz and carefully chosen epoxies should be used where maximizing light collection is desired. Windows are coupled to photomultipliers with a silicone coupling grease such as DC 20-057 or with a gel system such as Sylgard 184. Both these materials can be obtained with good transmission for thin layers. Integral Line detectors eliminate the window by using the photomultiplier tube as part of the hermetic enclosure.

Mechanical Considerations

The alkali halides under study are not considered strong materials and all are hygroscopic to some degree. A detector package must be designed which both gives protection from mechanical and thermal shock and provides a hermetic seal for the crystal. The choice of package material is sometimes dictated by the properties of the radiation to be detected.

The problem encountered with most packaging designs is the necessity of providing for rigid containment of the crystal to prevent motion during mechanical shock while also providing for the conflicting requirement of space for thermal expansion. Thermal expansion coefficients of the scintillators are about three times greater than most metals and six times greater than glass. The crystal must be allowed to expand relative to housing by inserting a spring or other compliant material in the package. The thermal expansion coefficient for CsI is approximately 5×10^{-5}/°K whereas aluminum, for example, has a coefficient of 2×10^{-5}/°K. The differential coefficient would then be 3×10^{-5}/°K. A temperature change of 293°K would produce a differential expansion of 0.018 cm for a 30-cm (~ 1-ft) length.

Where a crystal is fastened to a glass window, the compliance of the coupling medium (e.g., epoxy) over the temperature range encountered must be taken into account. Crystal-glass interfaces of 0.76 mm (30-mil) thickness with silicone-type bonding materials can provide sufficient shear compliance over the temperature range of 213°K to 423°K to avoid crystal fracture stresses.

The compliant preload on a crystal must equal the maximum g force in the direction considered. The crush strength or ultimate limits of the crystal may not be exceeded by the preload forces.

Where low accelerations are involved and weights are not important, mechanical springs are almost always used for obtaining desired preloads. Since a powder packing medium required for reflectivity is not compliant and is difficult to maintain in place, it is avoided wherever the packaging problem is severe, even at the expenses of degrading performance. Flexible materials, such as rubber with trapped air bubbles to supply bulk compliance, have been used successfully. Requirements that the package be hermetically sealed mean that all joints must be either soldered, welded, epoxied, or have O-ring seals.

When an epoxy is used it must be compliant enough not to chip or crack when subjected to lower temperature extremes. Epoxies are generally employed in assemblies used in environments above 273°K. The epoxy also must not char or lose strength at the high-temperature end of the range. Since epoxies are not impermeable to water vapor, the possibility of crystal hydration must be minimized for long-term use or storage of a detector in a humid environment by minimizing the area of epoxy seals.

A typical arrangement for sealing a glass window into a metal can is shown in Figure A-9. Where required for other reasons, glass to metal seals can be used.

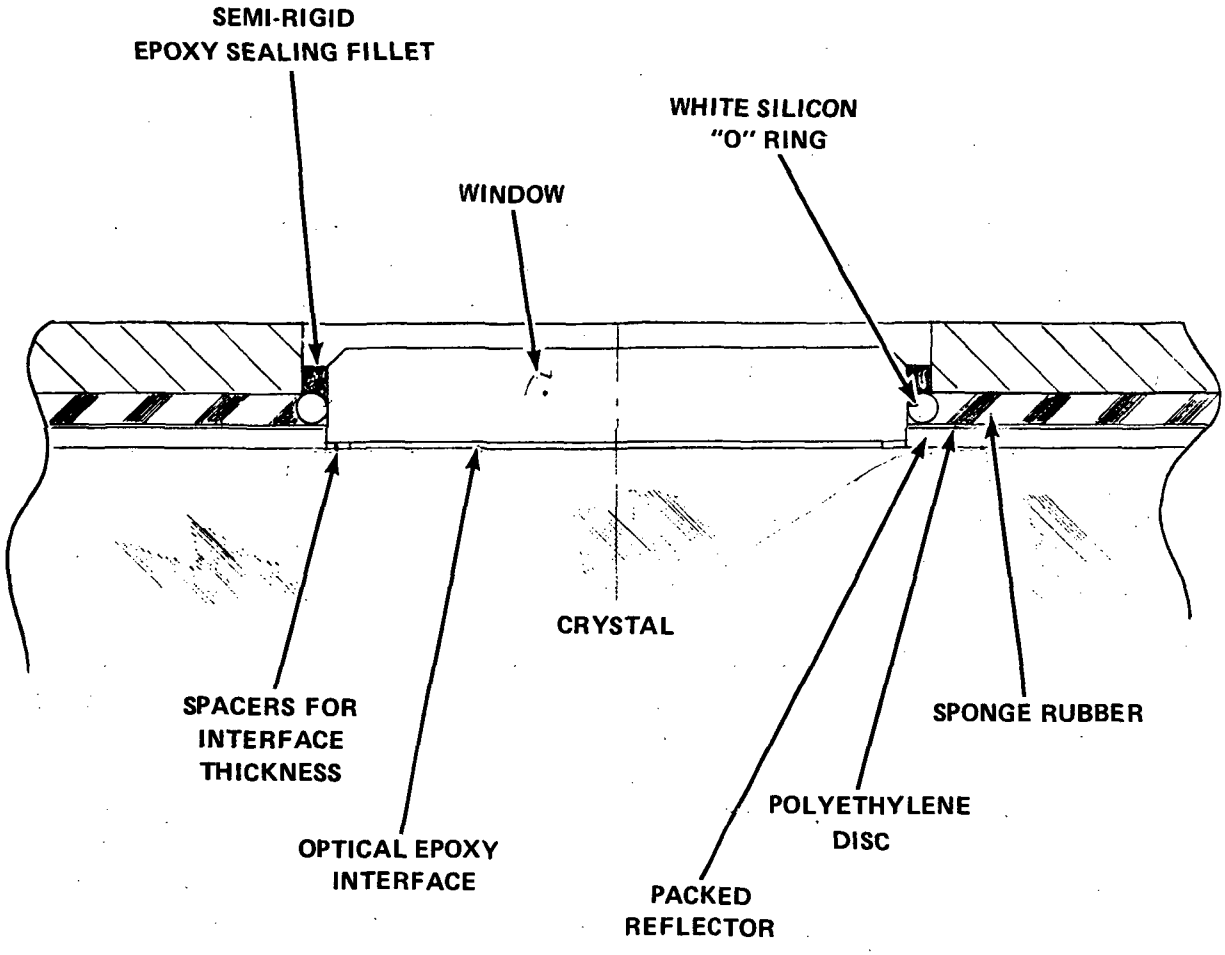

Figure A-9. Typical window configuration.

The advent of polycrystalline scintillators has provided the detector design engineer with several degrees of freedom heretofore not available. An almost unlimited variety of shapes and sizes or detectors is now possible in addition to a vast improvement in ruggedness in terms of resistance to thermal and mechanical shock.

Because of the natural cleavage planes present in single crystal NaI(Tℓ), crystal cracking in the single crystal material can never be completely avoided. Ultimate degradation of pulse height and resolution will depend on the degree and orientation of the fracture. By comparison, the resistance to cleavage of the Polyscin materials means greater freedom from resolution loss caused by

crystal cracking. In addition, it is now possible to "spring load" crystals to higher levels, producing stronger detector packages. This, of course, is especially important where the detector is subjected to high g forces.

Page intentionally left blank

APPENDIX B

SURFACE PREPARATION AND REFLECTIVE COATING CONSIDERATIONS FOR CsI(Na) SCINTILLATOR SHIELD CRYSTALS

By

University of California, San Diego
Department of Physics,
X-Ray and γ-Ray Astronomy
La Jolla, California 92037

Page intentionally left blank

APPENDIX B

SURFACE PREPARATION AND REFLECTIVE COATING CONSIDERATIONS FOR CsI(Na) SCINTILLATOR SHIELD CRYSTALS

Introduction

The efficient use of scintillator shield crystals of complex geometry implies that the most optimum methods must be used to insure that light generated by events within the crystal reaches the photomultiplier detector and the subsequent signal chain. The investigation was undertaken to achieve this end within the constraints of the instrument design.

The problem was the determination of the best practical reflective surface preparation for CsI(Na) shield crystals for the HEAO experiment.

Physical Constraints

The physical constraints of self-absorption and light-trapping are discussed on the following pages.

Self-Absorption. This should be negligible in impurity-activated alkali halide crystals because the lattice is transparent to the activator emission. Close attention to the purity of the constituents, zone refining, and the exclusion of all extraneous impurities is necessary to insure this.

Light-Trapping. The extraction of the maximum number of photons from a scintillation is impeded by internal reflections at the surface. At a refractive index of approximately 1.5, only approximately 4 percent of the light intensity incident normal to the surface is reflected. As the angle of incidence is increased, reflectivity increases and becomes 100 percent when the critical angle ($\sim$ 45 deg) is reached. Only the light in this semi-angle can escape to the outside. In the simple geometry of a rectangular parallelpiped, the escaped light (for NaI) would be 8.9 percent from each of the six surfaces, the remaining 47.5 percent being internally trapped. If one surface is covered with aluminum foil, the light at the opposite surface is nearly doubled. Returning more light to a given surface in complex geometries is thus much more complicated. Light-trapping may be reduced by introducing diffuse reflection by roughening all crystal surfaces other than those coupled to the detectors or

by coating the surface with a diffuse reflector. Any medium imposed between the crystal surface and reflector can only decrease the reflectivity.

Reflectors. Aluminum foil or evaporated aluminum is the best specular reflector in the region of scintillator emission. It has a reflectivity of approximately 90 percent down to 300 μm λ. The diffuse reflectivity of several dry reflectors relative to aluminum foil is shown in the following table.

	At 400 nm (4000 Å) (%)	At 500 nm (5000 Å) (%)
α Alumina (Linde A)	~ 96	~ 94
Magnesium Oxide (Baker reagent)	~ 95	~ 96
α Alumina (sprayed with sodium silicate binder)	~ 93	
Alumina Foil (dull side)	~ 90	
Tygon Paint (T_1O_2)	~ 70	

Although MgO_2 has slightly better reflectivity at longer wavelengths, it is more affected by oils and is therefore less preferred than $A\ell_2O_3$. $XA\ell_2O_3$ + sodium silicate sprayed on Hℓ foil and tightly applied to the crystal surface by pressure has been successfully used as a reflective medium and the $A\ell_2O_3$ dry powder pack method is the standard commercial packaging method.

Experimental data to determine the correctness of the preceding tabulation have been obtained on the materials in the following table showing relative results.

Material	Relative Reflectivity (%)
MgO	100
$A\ell_2O_3$	96.5
Aℓ Foil	72
Aℓ Foil with Sylgard 184 Adhesive	61.5

These follow the expected results for published reflectivities for these materials, including the behavior of binding mediums on the destruction of reflective power. Further experimental data will be obtained for materials which can be made cohesive with the crystal surface such as high-reflectivity paints,

aluminum (either flame sprayed or vacuum deposited), and elastomers with high-reflectivity pigments.

Method of Measurement. A 7.6-cm-by-7.6-cm (3-in.-by-3-in.) CsI (Na) crystal cemented to a Lucite window, which can be grease-coupled to a photomultiplier tube and provided with a snap-on can to hold the powders, was used in a standard scintillation detector - pulse height analyzer arrangement. All operating conditions remained fixed and the keV/ channel change for several radio sources was the basis for the evaluation. The results are plotted in Figure B-1.

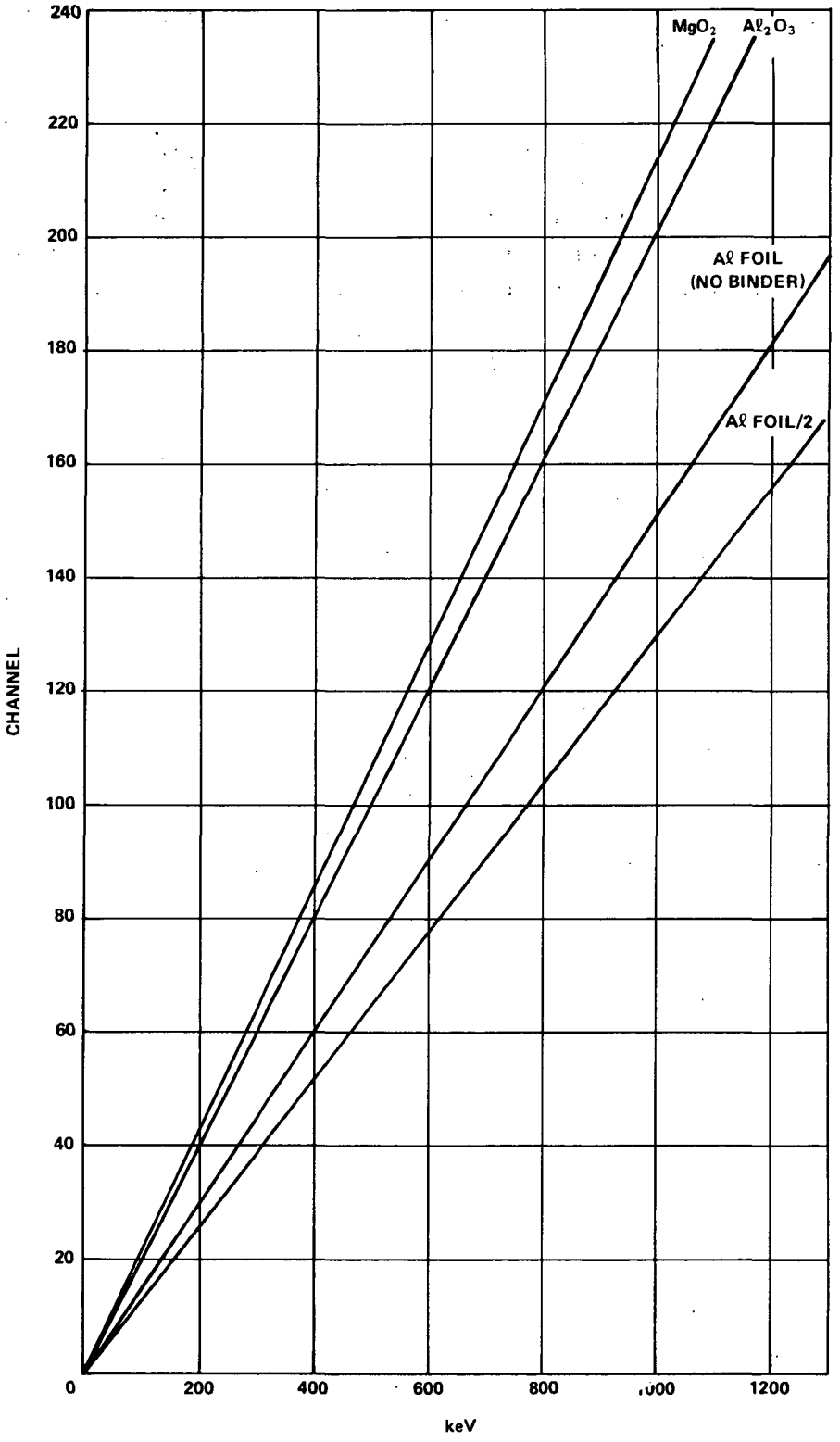

Figure B-1. Change in keV/channel as a function of reflective material.

APPENDIX C

INTERIM REPORT ON THE CsI DETECTOR FOR EXPERIMENT ACR-6 ON ORIGINAL HEAO-A

By

Carol Jo Crannell and Jane Jellison
Goddard Space Flight Center
Materials Engineering Branch
Greenbelt, Maryland 20771

Page intentionally left blank

APPENDIX C

INTERIM REPORT ON THE CsI DETECTOR FOR EXPERIMENT ACR-6 ON ORIGINAL HEAO-A

Introduction

A year ago Jon Ormes asked this author (Carol Jo Crannell) to take charge of the activities at the Goddard Space Flight Center (GSFC) relating to the CsI detector until our HEAO-A collaborators from the Max Planck Institut (MPI) arrived and assumed that responsibility. Recently both Wolfgang Schmidt and Manfred Simon have arrived from MPI. This report presents the information gathered to date from many helpful sources, the measurements and tests performed by GSFC personnel and colleagues, the work in progress, and the efforts planned for the CsI detector. Much of the information in this report is already known by those who will receive it or was, in fact, obtained from them. Still more of the information, however, is written only in data books or in notes from telephone conversations. I hope that not only will the data be useful but also that the conclusions, while preliminary, will help to clarify our understanding of the material and of the detector response with which we are working.

Objectives

The CsI detector is designed to be the primary portion of the ionization spectrometer from which can be obtained unambiguous identification of cosmic ray electrons, separating them from the copious proton background. Since the CsI detector is made up of five modules, each 1 radiation length thick and totally active, it will also provide most of the information on the electron energy spectrum. Detailed data on the development of electromagnetic cascades will be obtained by independent pulse height analysis on each of the five modules. Originally we hoped to obtain additional information from some or all of the modules by pulse shape analysis as well.

In our activities, all of which have been prior to purchasing the CsI material, we have attempted to define the handling procedure, the packaging configuration and techniques, and the mechanical and structural configuration for the CsI assembly. From these and other considerations we have been assisting our MPI collaborators in writing the purchasing specifications based

on performance requirements. We have obtained mechanical data from Marshall Space Flight Center (MSFC), and we have measured the effects of optical clarity and polish at GSFC. Scintillation response has been studied as a function of activator, of photomultiplier tube (PMT), and of area response using radioactive sources, cosmic ray muons, and accelerator particles.

Handling Procedures

Handling procedures are being defined with the consultation of M. R. Farukhi and E. Schraeder of Harshaw Chemical Company. Polishing techniques have been obtained, also with Harshaw consultation, by John Tarpley and further refined by Jane Jellison, both of GSFC. She wrote the cesium iodide polishing prescription given in the last section of this appendix.

Since CsI is a salt, it dissolves on contact with moisture. It should never be touched with bare hands and according to Schraeder, it should never be exposed to an atmosphere with relative humidity such that the dew point is at a temperature higher than 278°K. CsI(Tℓ) presents a personnel danger in that the Tℓ can produce heavy metal poisoning by absorption through the skin. CsI(Na) is even more critically sensitive to moisture damage because of the chemically active nature of the Na. According to Farukhi, the Na forms NaOH, thereby deactivating the scintillation dopant. Our observations are consistent with that description. CsI is soft and easily marred with scratches. The material tends to cold flow and except for Polyscin is flexible like lead. It is best handled only on smooth, flat, dry surfaces, which does not include being picked up by finger pressure through a plastic bag.

Encapsulation

To protect the CsI material, each of our modules will be individually encapsulated in plastic much as were the samples prepared and calibrated by our collaborators at Louisiana State University (LSU). John Tarpley has selected the materials: silica oil, UVT plexiglass, and ethylene dichloride for solvent bonding, which are optically desirable and low outgassing. Harry Nichols of GSFC has designed the mechanical structure to hold and support the five modules. He has also designed the aluminum light guides and a light maze which will couple the guide to the PMT housing.

Dr. Robert Snyder and his group at MSFC have reported on mechanical tests performed on a variety of CsI samples obtained from two companies, Harshaw and Teledyne Isotopes. Through Norman Levine of MSFC, we have

obtained a sample of CsI(Tℓ) of dimensions 1.9 by 23 by 23 cm^3 to test our encapsulation procedure, to check optical performance, and to study scintillation response. The piece was polished first by Teledyne Isotopes, at which time a crack developed. It was polished further by Jane Jellison, and the piece separated at the crack. In spite of the crack, it was encapsulated as a unit in plastic with 60 g of silica oil. It has been thermal-cycled from 253°K to 313°K and held for extended periods at each extreme with no adverse effects apparent. The resolution of the encapsulated piece in response to cosmic ray muons was measured before the thermal cycling with a mockup light guide. This author studied the area response by moving a counter telescope, in coincidence with the CsI signals, as indicated in Figure C-1. The relative response, as given by the peak channel in a pulse height distribution, and the resolution are also presented. The results are surprising and are being studied further by Eric Arens of GSFC and Gordon Vaughn-Cooke of Federal City College (FCC), Washington, D.C., using ray tracing. It is planned to repeat the measurements after thermal and thermal-vacuum cycling to test for degradation in any of the detector materials.

Optical Properties

Eric Arens has enlisted the support of Walter Viehmann of GSFC and Haven Whiteside of FCC to measure the optical properties of CsI as a function of several significant parameters. A small cylindrical sample of CsI(Tℓ) was obtained from Harshaw more than 2 years ago. This piece, identified as "Arlene's," has subsequently been chipped (intentionally by this author), had a flat cut along the cylinder, and been polished by Jane Jellison. The piece identified as "Isotopes/Marshall" was used to study transmission as a function of the number of reflections, both before and after encapsulation. With the large piece of encapsulated CsI(Tℓ), Haven Whiteside observed that transmission normal to the crack was not significantly worse than across other paths through the piece. This observation is surprising but consistent with the similarly surprising resolution measurements. Two small rectangular samples of CsI(Na), Polyscin, were obtained from Harshaw on August 18, 1972. They were polished on all surfaces by Harshaw. Transmission measurements on these pieces were made 6 days later by Walter Viehmann and for comparison on "Arlene's" CsI(Tℓ). A description of these measurements will be presented in a report currently being prepared by Walter Viehmann. The results of the transmission measurements are summarized in Tables C-1 and C-2.

These results indicate that the surface condition is very important for unencapsulated pieces. Also indicated is that encapsulation helps both in

getting the light out and in approaching total internal reflection along the reflecting surfaces. Internal reflection is improved because of the good surface of the plastic.

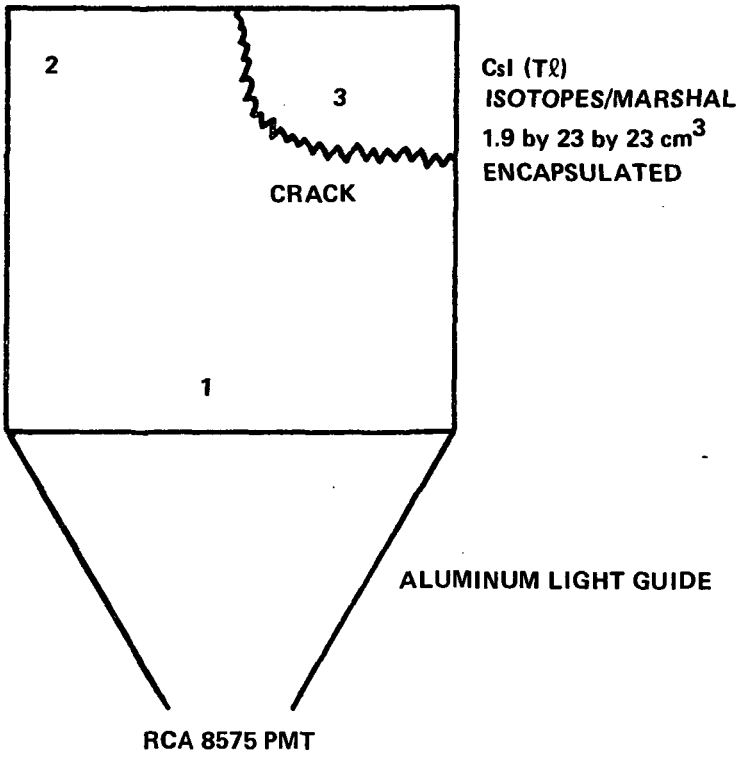

Run No.	Peak Channel	Resolution (%)
1	48	50
2	68	42
3	68	45

NOTE: ***Measurements were repeated with the scintillator rotated 90 deg with respect to the PMT and with lower PMT high voltage. The same results relative to the geometrical configuration were obtained.***

Figure C-1. Illustration of resolution measurements and results.

TABLE C-1. TRANSMISSION MEASUREMENTS (T) FOR NORMAL INCIDENCE

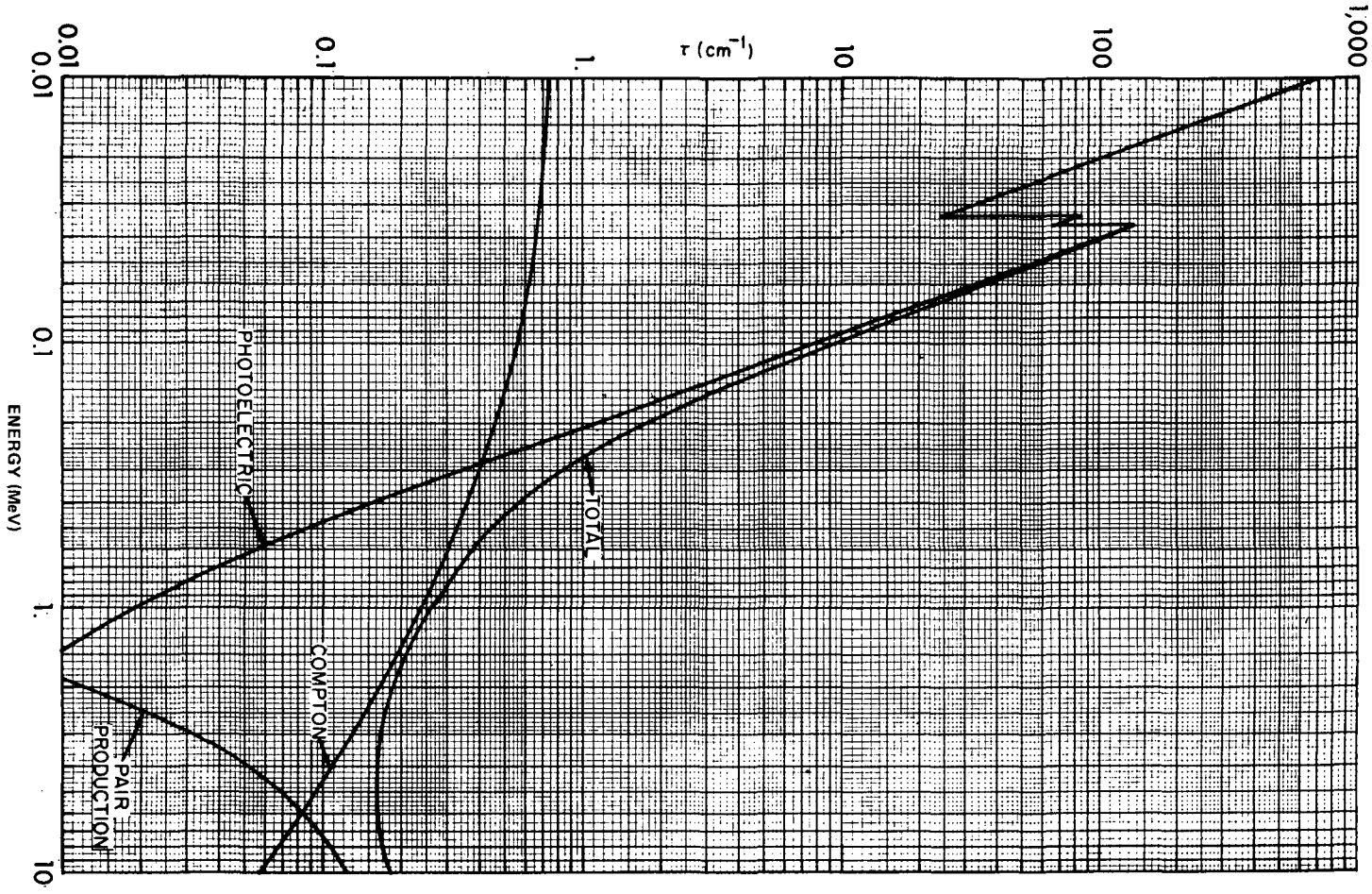

TABLE C-2. TRANSMISSION MEASUREMENTS (T_N) FOR N REFLECTIONS

λ = 633 nm	CsI, "Single" Crystal 2.7 cm Tℓ-Doped (Arlene's)		Marshall/Isotopes "Single" Crystal 23 cm		Polyscin 5 cm Sample No. 1		Polyscin 6.4 cm Sample No. 3		Lucite	
	Unencap.	Encap.	Unencap.	Encap.	Unencap.	Encap.	Unencap.	Encap.	33 cm[a]	0.2 cm
Cary 14 $\frac{T(meas)}{T(calc)}$ Normal	75% S_1=14%	87% S_1=7%			74% S_1=14%	82% S_1=9.5%	60% S_1=22%	82% S_1=9.5%		95% S_1=2.5%
Laser $\frac{T(meas)}{T(calc)}$ Normal	85% S_1=8%	95% S_1=2.5%	76% S_1=13%	92% $S_1 \approx 4\%$	80% S_1=10.5%	94% S_1=3%			76% $S_1 \approx 13\%$	98% S_1=1%
Laser $T_{10}/T(norm)$ Measured			$\leq 1\%$ $S_2 \geq 20\%$	30% $S_2 \approx 10\%$					57% $S_2 \approx 5\%$	
$T_{10}/T(norm)$ Calculated			90%	86%					98%	
$\frac{T_{10}/T(norm) \text{ Measured}}{T_{10}/T(norm) \text{ Calculated}}$			<0.01	0.35						0.58

a. Considerable volume scattering observed in this particular sample.

The quality of the Polyscin is quite variable and while much of the poor transmission is due to poor surface quality, significant volume absorption cannot be ruled out. Harshaw reports difficulty (which it believes it can now overcome) in polishing the smaller surfaces of CsI Polyscin because of chipping along the sharp edges.

Scintillation Response

The useful signal from scintillation phosphor depends on the fold of the frequency response function of the scintillator with the frequency response function of the associated PMT's. The PMT's under consideration for use on the present HEAO-A experiment have a peak response in the blue region of the spectrum. Samples of CsI(Na) and CsI(Tℓ) were tested with one of these PMT's, an RCA 8575. The signal from the CsI(Na) was approximately twice the size of the signal from the CsI(Tℓ) for α-particle irradiation. This observation is consistent with the spectral response functions reported in the literature [2] and measured with the same two scintillator samples by Walter Viehmann. CsI(Na) peaks in the blue so that its response more nearly matches the sensitivity of the PMT. CsI(Tℓ) exhibits a broader response function which peaks in the yellow.

Pulse Shape Discrimination (PSD) – Characteristics

At the suggestion of our collaborators at LSU, studies were undertaken to determine the time dependence of CsI scintillation response on the characteristics of the stimulating radiation. Richard Kurz, formerly of the Manned Spacecraft Center in Houston and now at TRW in San Diego, distributed a summary of his literature search. The draft, dated January 10, 1972, contains an extensive bibliography on both general and pulse-shaped characteristics of CsI(Tℓ). At the end of this report are two additional references [2,3] which are the interesting sources of information this author found not referenced by Kurz.

The time dependence of the response of CsI(Tℓ) and of CsI(Na) coupled to an RCA 8575 PMT and to an Amperex 56 AVP were measured for a variety of incident radiation. The cathodes of the PMT's were held at negative high voltage, and the anode pulses were direct coupled to an oscilloscope input through a 50 termination. The experimental configurations investigated and the time constants obtained to date are summarized in Table C-3. Graphs of some of the pulses and composite pulses are also given in Figure C-2.

TABLE C-3. TIME CONSTANT OF THE DECAY OF SCINTILLATION RESPONSE

Measured at GSFC		
Detector Assembly	Incident μ	Radiation α
CsI(Tℓ) RCA 8575 PMT Amperex 56 AVP	 0.6 0.7	 0.5
Measured at Brookhaven National Laboratory		
	Noninteracting 14-GeV π^-	Interacting 14-GeV π^-
CsI(Tℓ) RCA 8575 PMT Amperex 56 AVP CsI(Na) RCA 8575 PMT Amperex 56 AVP	 0.6 X X X	 X X X X
Other (From Ref. 4)		
	0.66 MeV e	4.8 MeV α
CsI(Tℓ) DuMont 6292	 0.695	 0.423

The time constant obtained from cosmic ray muons, incident on CsI(Tℓ), coupled to an Amperex 56 AVP, agrees with the measurements reported by Storey, Jack, and Ward [4], also presented in Table C-3. CsI(Tℓ) was coupled to an RCA 8575; however, the observed time constant associated with cosmic ray muons was considerably shorter. Numerous experimental checks were made to insure that the time constants were dominated by the scintillator-PMT response and not by the oscilloscope nor by saturation effects in the PMT. The difference is apparently due to the difference in spectral response of the two PMT's. Further investigations are planned using a very broad-spectrum response PMT with optical filters and spectrographs.

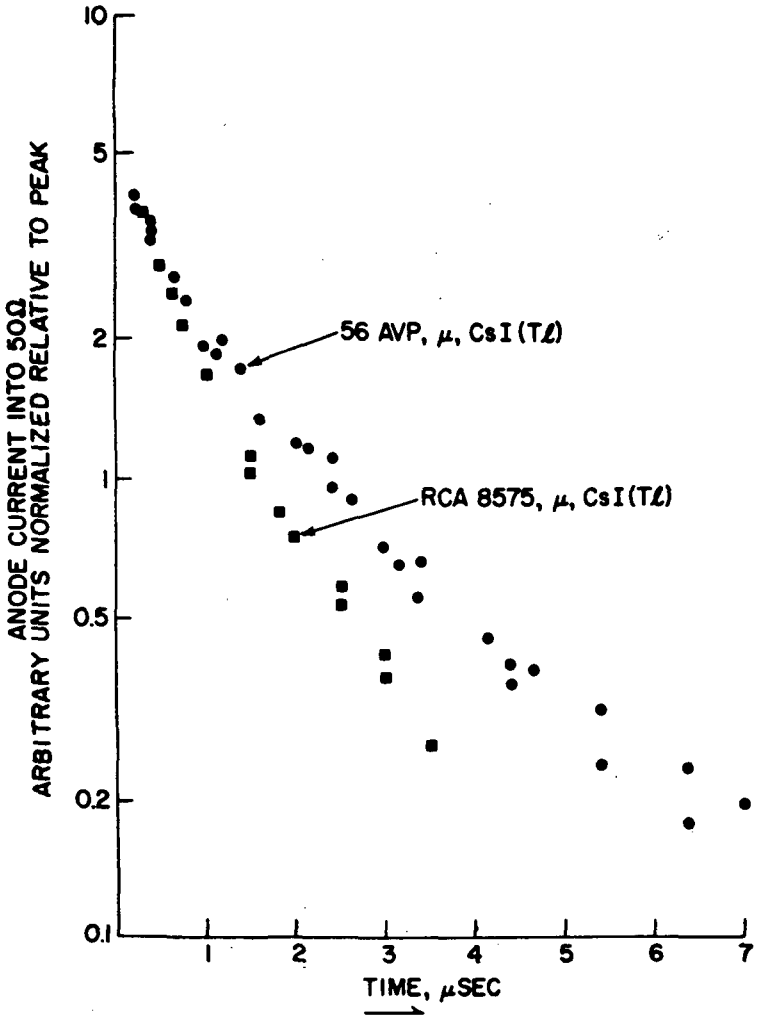

a.

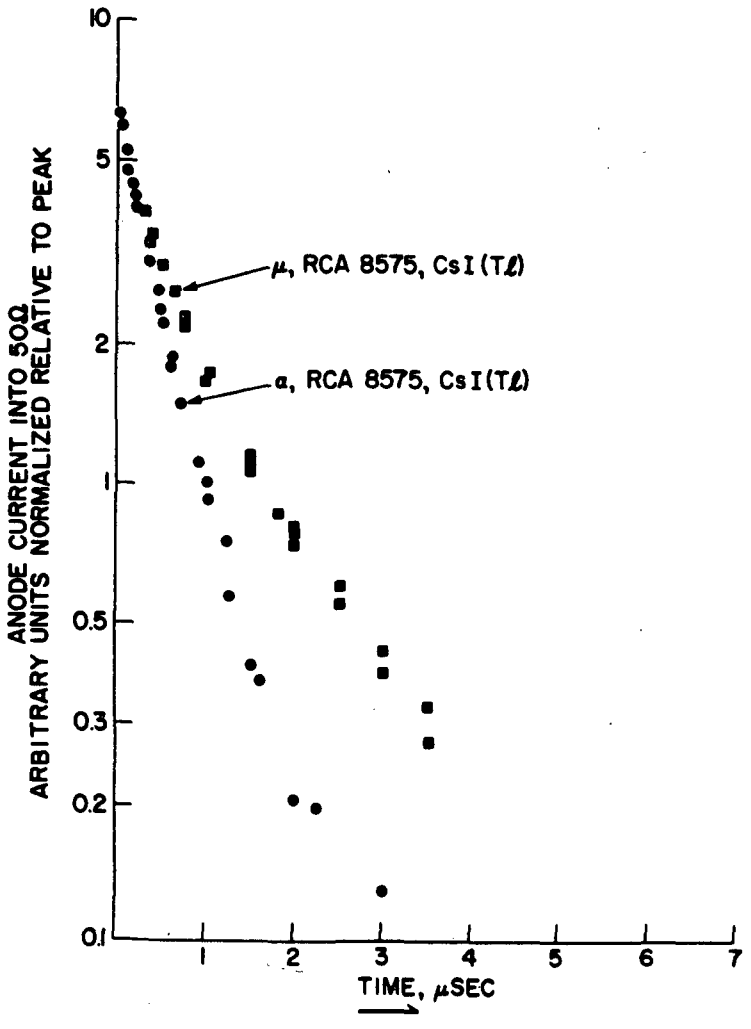

b.

Figure C-2. Time-dependent response curves.

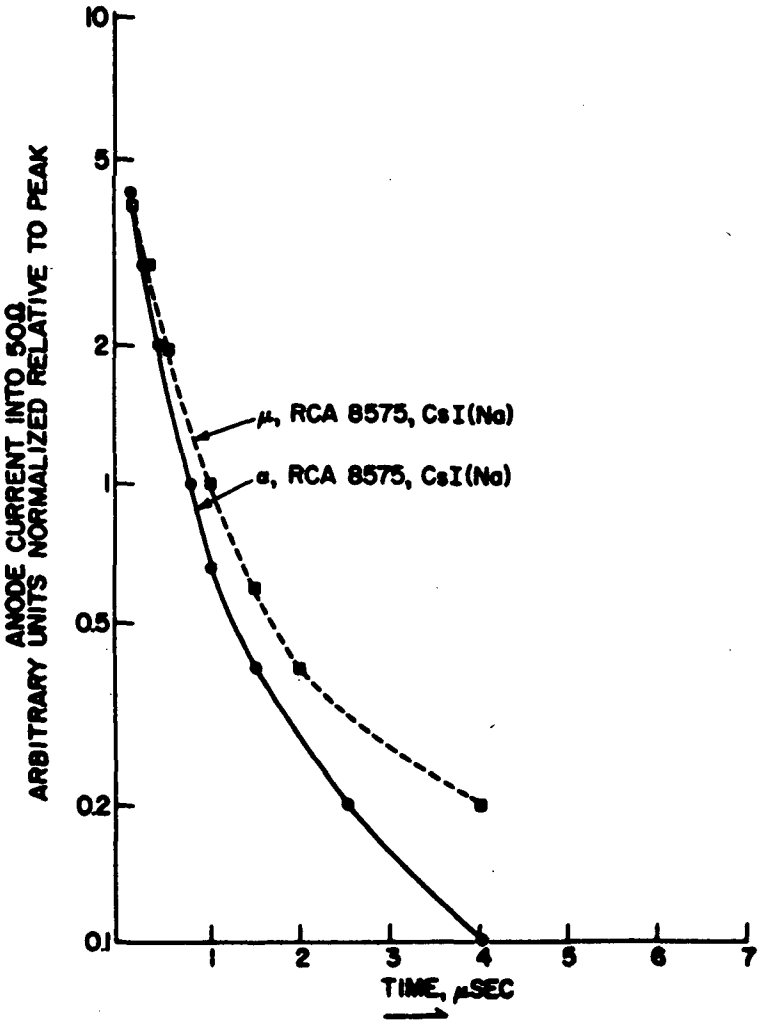

c.

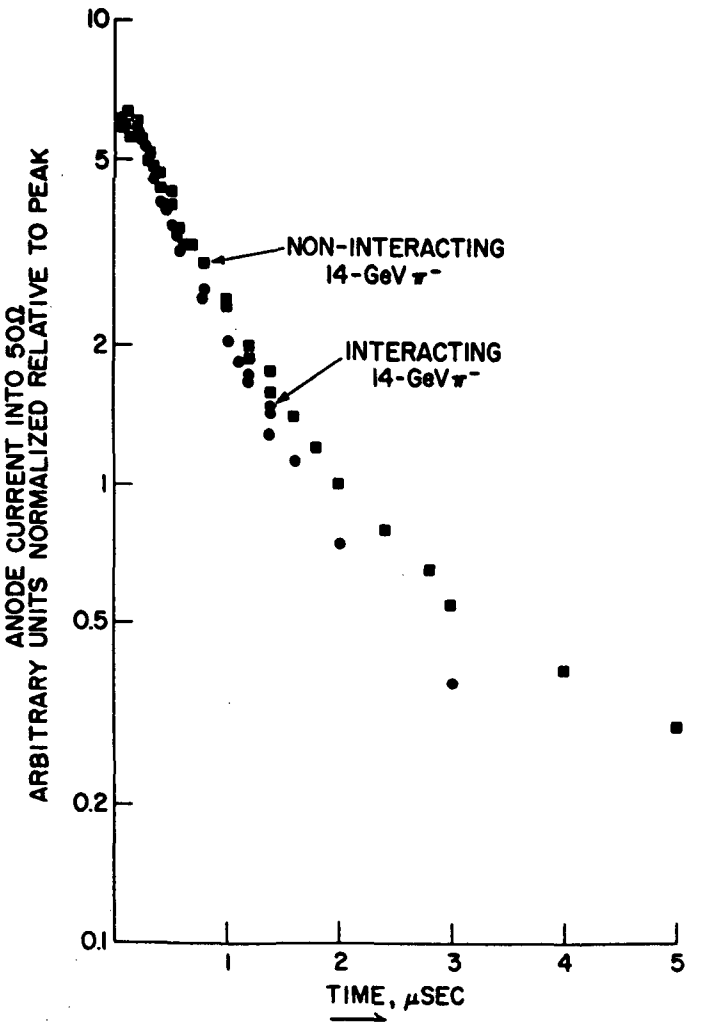

d.

Figure C-2. (Concluded).

The first attempt to measure the difference between the pulse shapes for cosmic ray muon and for α-particle irradiation was made with a CsI(Tℓ) sample coupled to an RCA 8575 PMT. The measured pulse shapes are illustrated in Figure C-2b. The time constants are not consistent with those reported by Storey, Jack, and Ward [4] but, in fact, show less pulse-shaped discrimination. It is hoped that investigations of the spectral dependence of the pulse shapes will indicate an optimal spectral band in which to discriminate between ionization energy deposit caused by relativistic singly charged particles and that caused by more highly ionizing radiation.

The second attempt, with a CsI(Na) sample and an RCA 8575, gave results with approximately the reported C time constant for cosmic ray muons, but with a very strange pulse for α-particle irradiation. The pulses were an order of magnitude smaller than expected and of only 30-nsec duration. A guess was made that the observations were related to hydration of the Na dopant in the surface. To test this hypothesis the CsI(Na) sample was removed from the PMT, chipped, and replaced with the α-particle source on the freshly exposed surface. The pulses observed for the next several hours appeared as had been originally expected but in 4 days' time were predominantly of the variety first observed. The CsI(Na) sample obtained from Harshaw, sealed in a plastic bag with a dessicant, exhibited the small, fast pulses in response to α-particle irradiation within minutes after removal from the sealed bag. In consultation with Harshaw, it was concluded that the small, fast pulses are the scintillation response of undoped CsI which is effectively obtained in the surface of CsI(Na) by removal of the activator through NaOH formation. For use in pulse-shape discrimination, the CsI(Na) shows less difference between muon and α stimulation than does a similar sample of CsI(Tℓ) when the surface problem is eliminated (compare Fig. C-2c with Fig. C-2b).

As a further check on the measurements, "Arlene's" CsI(Tℓ) sample was chipped and the α-particle source placed on the fresh surface. The observed pulses were the same as those obtained previously with that sample.

Since the proposed use of PSD is to assist in identifying interacting cosmic ray photons, the response of the Harshaw CsI(Tℓ) and CsI(Na) samples was measured at Brookhaven National Laboratory using 14-GeV π^- from the G-10, +4.7-deg test beam of the alternating gradient synchrotron (AGS). Andrew Fisher, NAS/NRC fellow at GSFC; Hall Crannell, professor of physics at Catholic University; and Gordon Vaughn-Cooke, a student at Federal City College, assisted this author in making the measurements. The first data to be reduced since the measurements were made in August are shown in Figure C-2d. The PSD is small but significant, and it is hoped that the results can be both enhanced and utilized.

Pulse Shape Discrimination – Techniques

During the past year Alan Macnee, professor of electronics engineering at the University of Michigan, participated in the GSFC effort as a NAS/NRC senior research fellow. For PSD he developed a circuit which yields a null response for pulses slower than a predetermined rate of decay and which yields a pulse approximately proportional to the charge in the fast component of the pulse times the reciprocal of the time constant for those pulses which are faster. To fit the measured pulse shapes to an analytic form, Professor Macnee made available to us a FORTRAN program which fits the experimental data to a sum of from one to three independent exponential components. The circuit is still being improved to expand its dynamic range, and the program is being used to analyze the data discussed in the previous section.

An Ortec PSD system, utilizing a time to zero-cross technique, has been purchased. An extra pair of decay lines, to double the system time constant, has also been purchased to further optimize the PSD for use with most CsI pulses. Work on a variety of PSD techniques will continue in conjunction with the effort to achieve the greatest possible differences between pulse shapes due to singly ionizing particles and those due to more highly ionizing radiation.

Proposed Future Studies

A large sample of CsI(Na), Polyscin, also obtained through MSFC is being encapsulated to further test and refine the encapsulation procedure. The encapsulated piece will be subjected to transmission and reflection measurements described by Viehmann. With this sample and with the large, encapsulated CsI(Tℓ) sample, thermo-vacuum vibration tests will be performed. The temperature dependence of the scintillator response also needs to be determined. The tests will be followed by optical measurements to check for any degradation in performance. Use of a blue laser would enable tests of the optical transmission and reflection at a wavelength nearer that of the CsI emission. It is hoped that such a laser can soon be obtained.

Anton Scheepmaker of the Massachusetts Institute of Technology has ordered some 38-cm long, rectangular CsI rods: CsI(Na), regular, and Polyscin. We hope to compare the transmission and reflection properties of these samples using the GSFC equipment and techniques. Scheepmaker has also suggested to us the use of rough-cut Plexiglas on the viewing surface of the encapsulating material to minimize loss of light through internal reflections at

that surface. Tests of this and various lense-like surfaces are planned.

The material for the air-filled light guides is yet to be chosen. Which of the available surfaces provides the best resolution must be determined.

The time constant of the preamplifiers used with the CsI needs to be adjusted to be compatible with the long-duration CsI scintillation response. The optimization of the preamplifier time constant will be an important aspect in obtaining good single-particle resolution.

The use of PSD has been dropped from this HEAO-A experiment because of a need to economize both on personnel and on flight-qualified apparatus. This author will continue to investigate PSD, at a reduced priority level, in the hope that it can be made technologically useful either in similar or more advanced applications. One application could be on a balloon-borne experiment, the same geometrical and detector configuration as the present HEAO experiment. By correlating the PSD data so obtained with the pulse height data for those particles which satisfied the electron-trigger criteria, we could develop more sophisticated techniques for separating interacting protons from electrons. Either by balloon-borne cosmic ray measurements or by accelerator calibrations at high energies, tighter confidence limits could be put on the energy-dependence of the presently necessary statistical corrections for apparent proton contamination.

Polishing Cesium Iodide

Grinding. Coarse scratches are eliminated by using an appropriate grit size of emery paper moistened with ethylene glycol ($C_2H_6O_2$). Buehler 30-5024 4/0 grade (15-μm grit size) will remove all but very deep scratches. The ethylene glycol slightly attacks CsI and should not be allowed to stand on it very long. With this particular paper, the adhesive which bonds the abrasive to the paper will dissolve in the ethylene glycol, creating a brown slurry. A soft facial tissue moistened with ethylene glycol may be used to rub this slurry over the crystal.

When the coarse scratches have been removed, clean the crystal by wiping with a succession of clean tissues moistened with ethylene glycol. Then clean the ethylene glycol off with methyl alcohol applied with tissue.

Intermediate Polishing. Moisten a pad of facial tissue with ethylene glycol and sprinkle about 0.5 g or so of 0.3-μm $A\ell_2O_3$. Polish with this,

occasionally adding a little ethylene to the pad. Clean as before, with ethylene glycol followed by methyl alcohol. The finish will be hazy with very light scratches.

Final Polishing. Moisten a pad of tissue with methyl alcohol and sprinkle a small amount (~ 0.1 g) zinc oxide powder on it. Rub with fairly heavy pressure over a small area of the crystal at a time, allowing the surface to dry every few seconds. Gradually the haze will disappear. Use light pressure towards the end. It may be necessary to rewet the pad with a few drops of methanol. This final polishing procedure may have to be repeated one or more times before a haze-free finish is attained. No cleaning is necessary after this step.

Notes. At no point apply the solvent directly to the crystal; a spot will be etched where each drop falls. Dry grinding should be avoided. If the emery paper starts to drag, add a little more ethylene glycol. Fingerprints will etch the crystal rather deeply; therefore, rubber surgical-type gloves are recommended. Change gloves, or wash them well with methyl alcohol, between the aluminum oxide and zinc oxide polishing steps. Avoid breathing on the polished surface when examining it closely. Store the polished crystals in a vacuum or in an inert gas mixture.

APPENDIX D

SCINTILLATION PERFORMANCE REPORT OF CsI(Tl) SLAB ASSEMBLIES

Prepared by

The Harshaw Chemical Company
Division of Kewanee Oil Company
Crystal & Electronic Products Dept.
Solon, Ohio 44139

for

National Aeronautics and Space Administration
George C. Marshall Space Flight Center
Marshall Space Flight Center, Alabama 35812

Under Contract NAS8-27893
Modification No. 2

Page intentionally left blank

APPENDIX D

SCINTILLATION PERFORMANCE REPORT OF CsI(Tl) SLAB ASSEMBLIES

Introduction

This is a report of a limited investigation undertaken at the request of the NASA-Marshall Space Flight Center under contract NAS8-27893.

In missions HEAO-A and HEAO-B, slabs (a "slab" is a parallelopiped, one dimension of which is small compared with the other two) of CsI(Tℓ) and CsI(Na) are being used as part of either an active collimator or of a Total Absorption Shower Counter (TASC). In either application, it is necessary to detect the scintillation light produced by the passage of an energetic charged particle passing through the slab of the scintillator. The geometry dictates that the light must be viewed through the edges of the slab. The purpose of this investigation was to determine the efficiency and uniformity of light collection and the effects on these quantities of various parameters. This investigation by no means exhausts the possibilities but, it is hoped, is thorough enough to give designers some criteria on which to base the design of their apparatus.

Experimental Methods

The scintillation light output of four CsI(Tℓ) slabs 21 cm by 21 cm by 2.2 cm (8 1/4 in. by 8 1/4 in. by 7/8 in.) was studied by placing four Amperex XP1010 photomultipliers on the edges of each slab. Various coupling methods were used, including two different types of light pipes. (These will be described later.)

The electronics used to amplify the photomultiplier signals were a standard charge sensitive preamplifier, Harshaw NB-11; Double RC Clipped Amplifier, Harshaw NA-16; and a multichannel analyzer (MCA) Nuclear Data Model 2200 (4096 channel).

A block diagram of the apparatus is shown in Figure D-1 and the essential parameters of this equipment are given in Table D-1.

The high voltage of each XP1010 was adjusted so that the pulse heights of the 662 keV peak from Cs^{137} placed in the center of the slab was the same for

each tube. This adjustment could be made to within ± 2 percent by overlapping spectra stored in various sections of the analyzer.

Each slab-light pipe configuration was wrapped with bright aluminum foil and then sealed against light leaks with black electrical tape. The assembly was placed on a contour-cut pad of Styrofoam to support the photomultipliers and crystal in the same plane. This was necessary to assure that the grease interfaces between crystal, light pipes, and photomultipliers would remain intact. In most cases coupling was secured by Dow Corning 20-057 grease but in some cases Harshaw Crystal Bond 21-X was used.

The channel number of the MCA in which the peak of the spectrum from a collimated, Cs^{137}, 662 keV gamma source appeared was used as the measure of the scintillation response. The term, relative pulse height, is the ratio of the channel number to the channel number at the reference position. The source was placed at various positions on the face, i.e., the 21-cm-by-21-cm (8 1/4 in. by 8 1/4 in.) surface of the slabs. The source collimator was a 2.54-cm (1 in.)-diameter, 5.08-cm (2 in.)-long hole in a lead brick placed within 0.95 cm (3/8 in.) of the crystal. The area illuminated [approximately 3.02 cm (1 3/16 in.) in diameter] was deemed sufficiently small for this study because peak position was found to vary slowly with source position, and relative performance on the various photomultiplier configurations was the matter of importance.

Experimental Results

Measurements of the 662 keV peak position were made at 13 positions of the collimator on the face of each slab. These positions are shown in Figure D-2.

The first series of measurements was performed to determine if the intrinsic output of each slab was similar to the others and symmetric with respect to their centers. Four XP1010 photomultipliers were grease-coupled to the edges [2.2 cm (7/8 in.) thick] of the slabs at their centers (Fig. D-1). The excess photocathode area above and below the crystal was covered with bright aluminum foil. For this part of the study each slab was left unpolished with a rough-cut finish, which is uniform and somewhat dull. The relative pulse heights detailed in Table D-2 indicate that the slabs are symmetric with respect to light output to within ± 3 percent, and the resolution (FWHM) of 17 percent to 18 percent indicates a light output variation of less than 10 percent between slabs.

It can be seen that with configuration 1 the light collected varies about 20 percent between a corner position and a position directly opposite a tube. This result is not unexpected since light from near the corners must undergo many reflections and scatterings before it is collected in a photomultiplier.

A complete tabulation of the performance of the various configurations of light pipe and photomultipler positions is given in Table D-3. In all configurations the photomultiplier tubes are in the plane of the slab. All configurations have a fourfold axis of symmetry. The light outputs given are the average of the corner positions (1, 3, 11, 13) and the average of the positions (2, 6, 8, 12) 2.54 cm (1 in.) from the center of the edge. All these outputs are normalized to center peak position (7), defined as 1.0.

Discussion and Conclusions

The results in Table D-3 indicate that there are variations in relative pulse height of about 10 percent for such a slab when viewed with four photomultipliers. Polishing of the large faces helps somewhat, improving the uniformity by 4 percent over the same configuration unpolished. Polishing the edges of the slab probably would have improved collection, but this was not tried.

The data also show that light pipes help the uninformity of collection, with the best configuration of those investigated being the one with the photomultipliers at the corners looking at the edges of the completely enclosing light-pipe arrangement, configuration No. 7 (Fig. D-3). The resolutions and uniformity of this last configuration should be sufficient to make possible observations of cosmic ray shower development with a slab-type TASC.

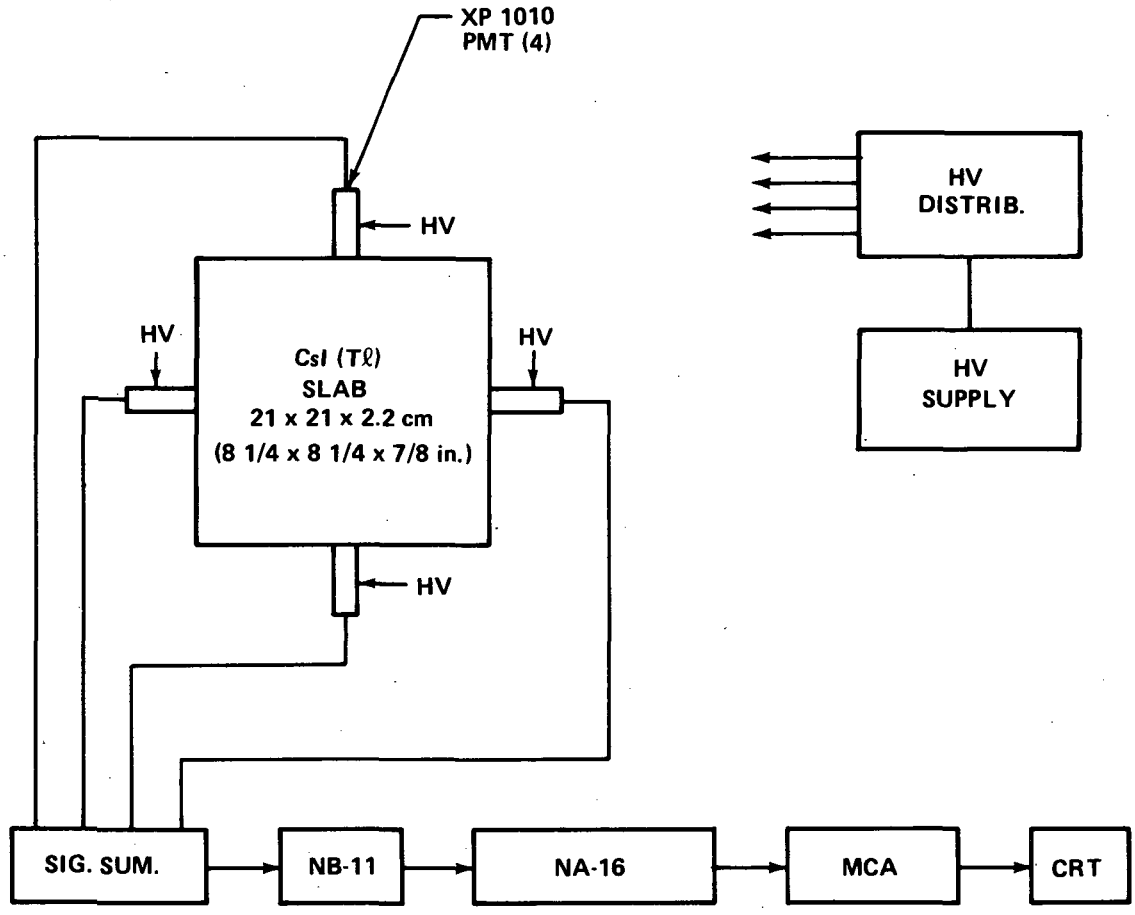

Figure D-1. Experimental arrangement for measuring scintillation performance of CsI(Tℓ) slabs.

TABLE D-1. AMPLIFIER EQUIPMENT

Equipment	Description
Harshaw NB-11	Charge Sensitive Preamplifier 100 μsec Clipping Time
Harshaw NA-16	Main Amplifier Double RC Clip Set at Differentiation: 1. 3.2 μsec 2. 3.2 μsec Integration 1.6 μsec
Nuclear Data 2200	+10-V Input 1024 Channels Used

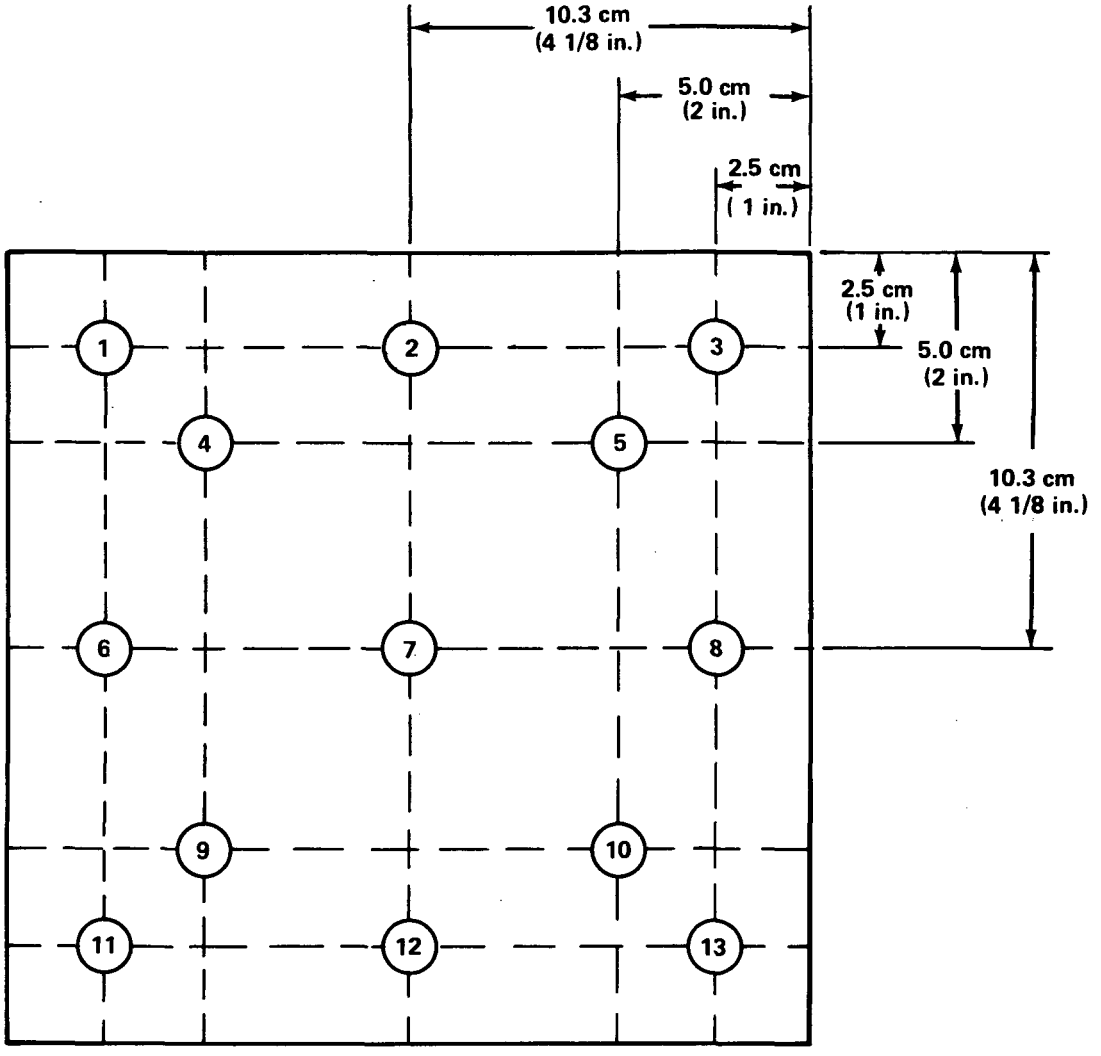

Figure D-2. Reference positions used in measuring scintillation performance of CsI(Tℓ) slabs.

TABLE D-2. RELATIVE PULSE HEIGHT[a]

Position No. (See Fig. D-2)	Slab No. 1	Slab No. 2	Slab No. 3	Slab No. 4
1	80	82	80	80
2	102	102	100	101
3	78	82	81	77
4	92	93	90	92
5	89	89	90	87
6	101	103	103	101
7	100	100	100	100
8	103	103	100	102
9	89	91	92	89
10	86	87	92	85
11	77	81	83	77
12	99	100	102	99
13	76	82	81	75

a. Pulse heights have been normalized to 100 at position No. 7 of each slab.

TABLE D-3. PERFORMANCE OF VARIOUS CONFIGURATIONS OF LIGHT PIPE AND PHOTOMULTIPLIER TUBE POSITIONS

Configuration No.	Description	Polish	Relative Pulse Height (See Text)
1	No light pipes; tubes grease-coupled to edges at center.	Dull, all surfaces	Center = 1.00 2.5 cm (1 in.) corner = 0.81 5.0 cm (2 in.) corner = 0.91 2.5 cm (1 in.) edge corner = 1.01 Cs^{137} resolution, 14.5%
2	No light pipes; tubes grease-coupled to edges at center but with 14 grooves cut 1.3 mm (50 mil) deep and 2.5 mm (100 mil) across edge under each tube.	Dull, all surfaces	Center = 1.00 2.5 cm (1 in.) corner = 0.80 5.0 cm (2 in.) corner = 0.96 2.5 cm (1 in.) edge center = 1.05 Cs^{137} resolution, 16.8%
3	Polished Lucite light pipes 21-X coupled along each slab edge. Tubes grease-coupled to center of each light pipe. Light pipes 1.9 cm × 2.2 cm × 22.9 cm (3/4 in. × 7/8 in. × 9 in.).	Large surfaces bright; edges dull	Center = 1.00 2.5 cm (1 in.) corner = 0.89 5.0 cm (2 in.) corner = 0.97 2.5 cm (1 in.) edge center = 1.04 Cs^{137} resolution, 17.3%
4	No light pipes; tubes grease-coupled to edges at center.	Same as No. 3	Center = 1.00 2.5 cm (1 in.) corner = 0.86 5.0 cm (2 in.) corner = 0.89 2.5 cm (1 in.) edge corner = 1.02 Cs^{137} resolution, 16.2%
5	No light pipes; tubes grease-coupled to edges adjacent to corners.	Same as No. 3	Center = 1.00 2.5 cm (1 in.) corner = 1.13 5.0 cm (2 in.) corner = 1.04 2.5 cm (1 in.) center of edge = 1.01 Cs^{137} resolution, 18.5%
6	Light pipes as in configuration No. 3 but with tubes coupled to ends of light pipes.	Same as No. 3	Center = 1.00 2.5 cm (1 in.) corner = 0.96 5.0 cm (2 in.) corner = 0.96 2.5 cm (1 in.) center of edge = 0.91 Cs^{137} resolution, 19.5%
7	Polished Lucite light pipes, 3.8 cm × 3.8 cm × 3.2 cm (1.5 in. × 1.5 in. × 1.25 in.) with right angle cut in 3.8 cm (1.5 in.) edge for corner of slab.	Same as No. 3	Center = 1.00 2.5 cm (1 in.) corner = 1.19 5.0 cm (2 in.) corner = 1.14 2.5 cm (1 in.) center of edge = 1.04

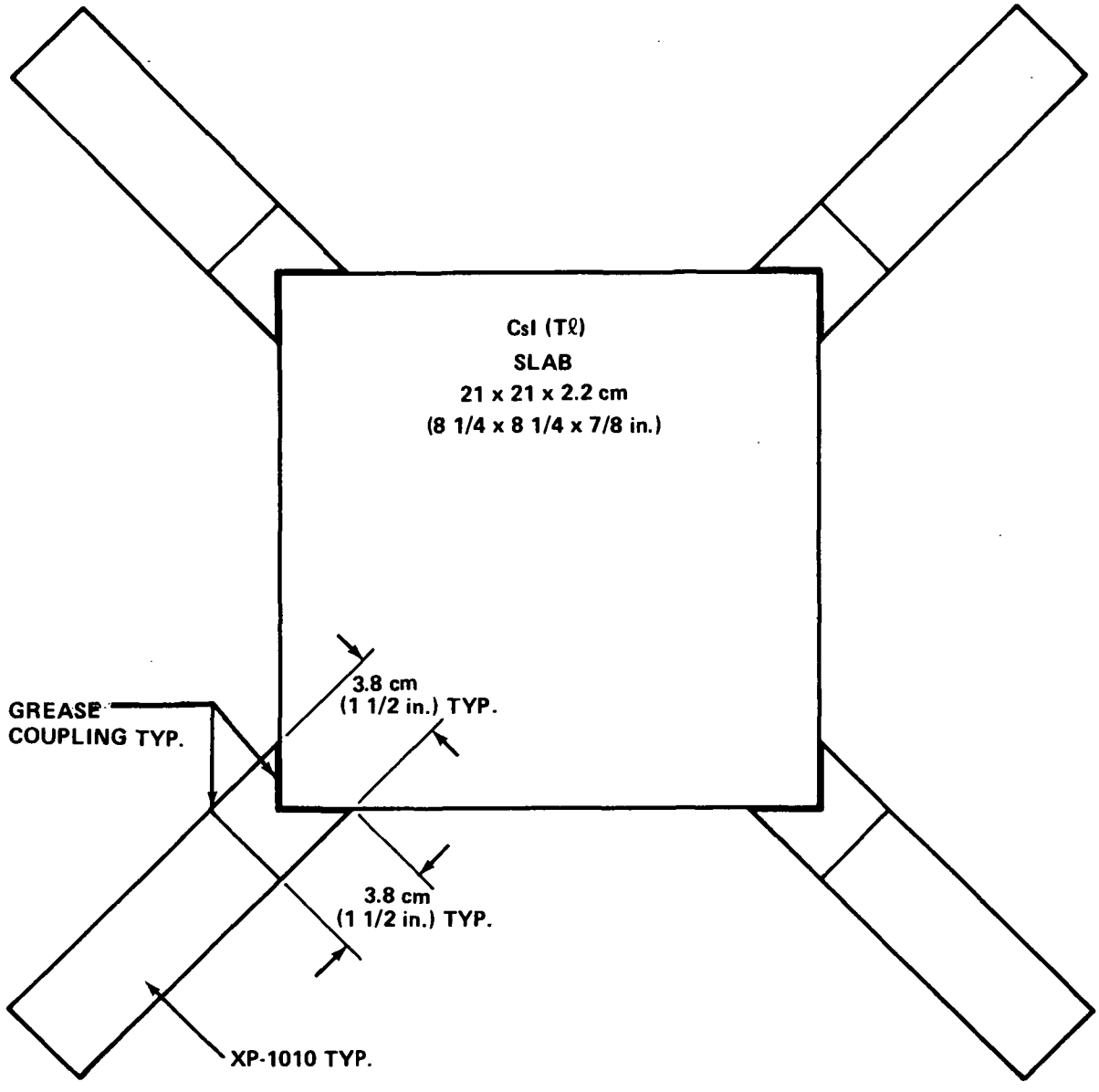

Figure D-3. CsI(Tℓ) slab with light pipes (configuration No. 7).

REFERENCES

1. McMaster, Robert C., ed.: Non-Destructive Testing Handbook. Ronald Press Co., New York, 1963.

2. Aitken, D. W.; Beron, B. L.; Yenicay, G.; and Zulliger, H. R.: The Fluorescent Response of Na(Tℓ), CsI(Na) and CaF(Eu) to X-Rays and Low Energy Gamma Rays. HEPL Report No. 478, Stanford University, 1966.

3. Keszthelyi-Landori, S.; and Hrehuss, G.: Scintillation Response Function and Decay Time of CsI(Na) to Charged Particles. Nuclear Instruments and Methods, Vol. 68, 1969, p. 9.

4. Storey, R. S.; Jack, W.; and Ward, A.: The Fluorescent Decay of CsI(Tℓ) for Particles of Different Ionization Density. Proceedings of the Physical Society (London), Vol. 72, 1958, p. 1.

APPROVAL

SCINTILLATOR HANDBOOK WITH EMPHASIS ON CESIUM IODIDE

By John L. Tidd, Joseph R. Dabbs, and Norman Levine

The information in this report has been reviewed for security classification. Review of any information concerning Department of Defense or Atomic Energy Commission programs has been made by the MSFC Security Classification Officer. This report, in its entirety, has been determined to be unclassified.

This document has also been reviewed and approved for technical accuracy.

for John O. Goodrum
JAMES T. MURPHY
Director, Program Development

F. Speer April 9, 1973
F. A. SPEER
Director, Space Science Projects Office

DISTRIBUTION

INTERNAL

DIR
Dr. Petrone

DEPT-T

A&PS-PAT
Mr. L. D. Wofford, Jr.

A&PS-MS-H

A&PS-MS-IP (2)

A&PS-MS-IL (8)

A&PS-TU (6)

A&PS-MS-D (25)

PD-DIR
Mr. J. Murphy

PD-MP
Mr. Joseph Dabbs (10)

PD-TR
Mr. John Tidd (10)

SS-DIR
Dr. F. Speer

SS-H-X
Mr. Norman Levine (20)
Mr. Carroll Dailey

S&E-SSL-NR
Dr. Thomas Parnell
Dr. Gerald Fishman

EXTERNAL

Space Science Division
Naval Research Laboratory
Washington, D.C. 20390
Attn: Dr. James Kurfess
William H. Conway

University of California, San Diego
P. O. Box 109
La Jolla, Ca. 92037
Attn: Dr. L. E. Peterson
Mr. Robert Farnsworth

Massachusetts Institute of Technology
Cambridge, Mass. 02139
Attn: Dr. Walter H. G. Lewin
Mr. John Barker
Room 37-627

NASA-Goddard Space Flight Center
Greenbelt, Md. 20771
Attn: Dr. Carl Fichtel
Dr. Jonathan Ormes
Dr. John Arens
Code 661

Space Science Division
Jet Propulsion Laboratory
4800 Oak Grove Drive
Pasadena, Ca. 91103
Attn: Dr. Allan S. Jacobson (2)

W. W. Hansen Laboratory
Stanford University
Stanford, Ca. 94305
Attn: Professor Robert Hofstadter
Dr. E. Barrie Hughes

Laboratory for Astrophysics and
Space Research
Enrico Fermi Institute
University of Chicago
Chicago, Ill. 60637
Attn: Mr. James Lamport (2)

TRW, Inc.
1 Space Park, Bldg. 0-1
Redondo Beach, Ca. 90278
Attn: Dr. R. J. Kurz
Dr. Robert Doolittle

Grumman Aerospace Corp.
Plant 25, Dept. 663
Bethpage, N. Y. 11714
Attn: Dr. Robert Madey

Harshaw Chemical Co.
6801 Cochran Road
Solon, Ohio 44139
Attn: Mr. David J. Krus (2)

Ball Brothers Research Corp.
Boulder Industrial Park
Boulder, Colo. 80302
Attn: Mr. D. B. Hicks (2)

Teledyne Isotopes
Westwood Laboratories
50 Van Buren Avenue
Westwood, N. J. 07675
Attn: Dr. M. R. Farukhi

Scientific and Technical
Information Facility (25)
P. O. Box 33
College Park, Md. 20740
Attn: NASA Rep. (S-AK/RKT)

Hayes International Corp.
HIC Building
Huntsville, Ala.
Attn: Mr. William T. Weissinger

Lawrence Berkeley Laboratory
University of California
Berkeley, Ca. 94720
Attn: Dr. Charles Orth/Bldg. 46

Quartz Products Corp.
P. O. Box 628
Plainfield, N. J. 07061
Attn: Mr. Norman Fein